

CONVERGENCE ANALYSIS FOR DEEP SPARSE CODING VIA CONVOLUTIONAL NEURAL NETWORKS

Jianfei Li*

Han Feng†

Ding-Xuan Zhou‡

December 2, 2024

ABSTRACT

In this work, we explore intersections between sparse coding and deep learning to enhance our understanding of feature extraction capabilities in advanced neural network architectures. We begin by introducing a novel class of Deep Sparse Coding (DSC) models and establish thorough theoretical analysis of their uniqueness and stability properties. By applying iterative algorithms to these DSC models, we derive convergence rates for convolutional neural networks (CNNs) in their ability to extract sparse features. This provides a strong theoretical foundation for the use of CNNs in sparse feature learning tasks. We additionally extend the convergence analysis to more general neural network architectures, including those with diverse activation functions, as well as self-attention and transformer-based models. This broadens the applicability of our findings to a wide range of deep learning methods for deep sparse feature extraction. Inspired by the strong connection between sparse coding and CNNs, we also explore training strategies to encourage neural networks to learn more sparse features. Through numerical experiments, we demonstrate the effectiveness of these approaches, providing valuable insights for the design of efficient and interpretable deep learning models.

Keywords deep learning; CNNs; sparse feature extraction.

1 Introduction

Convolutional neural networks (CNNs) have achieved remarkable successes in a wide range of computer vision and signal processing tasks, demonstrating their superior performances compared to traditional machine learning approaches. Theoretical insights to understand the ability of CNNs of learning effective feature representations from data are crucial for further advancing their capabilities and enabling their widespread adoption across various domains.

In the field of signal processing, the concept of sparse feature extraction has been recognized as a powerful technique for efficiently representing complex data. Sparse coding models aim to decompose signals into a linear combination of a small number of basis elements, enabling compact and informative feature representations. These sparse feature extraction methods have been extensively studied and applied in areas such as image denoising, compressed sensing, and dictionary learning.

The classical sparse coding algorithm is originally designed to represent data $\mathbf{y} \in \mathbb{R}^d$ into a sparse linear combination of a given dictionary $\mathbf{D} \in \mathbb{R}^{m \times d}$ by solving the following constrained optimization problem:

$$(P_0) \quad \min_{\mathbf{x}} \quad \|\mathbf{x}\|_0 \quad \text{s.t.} \quad \mathbf{y} = \mathbf{D}\mathbf{x},$$

where $\mathbf{x} := (x_i)_{i=1}^m \in \mathbb{R}^m$ and $\|\mathbf{x}\|_0 := \#\{i : x_i \neq 0\}$.

*Department of Mathematics, Ludwig-Maximilians-Universität München (lijianfei@math.lmu.de)

†Department of Mathematics, City University of Hong Kong (hanfeng@cityu.edu.hk)

‡School of Mathematics and Statistics, University of Sydney (dingxuan.zhou@sydney.edu.au)

Usually the strict constraint of (P_0) is relaxed with error-tolerance into account of noise involving in observation \mathbf{y} . Hence, instead, one may consider an error-tolerant version of (P_0) , by solving

$$(P_0^\varepsilon) \quad \min_{\mathbf{x}} \quad \|\mathbf{x}\|_0 \quad \text{s.t.} \quad \|\mathbf{y} - \mathbf{D}\mathbf{x}\|_2 \leq \varepsilon,$$

with $\varepsilon > 0$. Note that $\|\cdot\|_0$ is too sensitive to small entries and is not convex.

Consequently, to address the non-convexity and sensitivity issues of the ℓ_0 -based formulation, researchers have proposed alternative approaches that relax the ℓ_0 "norm" to the more tractable ℓ_1 norm. This has led to the well-known basis pursuit denoising (BPND) and least absolute shrinkage and selection operator (LASSO) problems, which can be formulated as the following variant with a regularization parameter $\lambda > 0$:

$$(P_{1,\lambda}) \quad \min_{\mathbf{x}} \quad \|\mathbf{x}\|_1 + \lambda \|\mathbf{y} - \mathbf{D}\mathbf{x}\|_2^2.$$

The ℓ_1 regularization term encourages sparse solutions, while the data fidelity term ensures the reconstructed signal $\mathbf{D}\mathbf{x}$ is close to the observed signal \mathbf{y} . This formulation has led to the development of many efficient algorithms for solving sparse coding problems, such as iterative shrinkage-thresholding algorithms (ISTA) and its accelerated variants.

One further variant of the sparse coding problem is the double-sparse coding framework, which was proposed by Rubinstein et al. [14] and further studied by Nguyen et al. [10]. In this formulation, the dictionary \mathbf{D} itself is assumed to have a sparse structure, expressed as: $\mathbf{D} = \mathbf{\Psi}\mathbf{A}$ where $\mathbf{\Psi} \in \mathbb{R}^{n \times n}$ is a "base dictionary" that is typically orthonormal (e.g., canonical or wavelet basis), and $\mathbf{A} \in \mathbb{R}^{n \times m}$ is a learned "synthesis" matrix whose columns are sparse. This double-sparse structure can provide additional flexibility and efficiency in representing the data, as the sparse columns of \mathbf{A} can be combined with the base dictionary $\mathbf{\Psi}$ to form the overall dictionary \mathbf{D} . The sparsity of \mathbf{A} also helps to reduce the number of parameters that need to be learned, making the model more interpretable and potentially more robust to overfitting.

Convolutional sparse coding (CSC) is another powerful extension of the standard sparse coding problem, which was first introduced by Zeiler et al. [21] in 2010. The key idea behind CSC is to leverage the convolutional structure of the dictionary \mathbf{D} to enable the unsupervised construction of hierarchical image representations. By restricting the dictionary to a convolutional form, CSC models can effectively capture the spatially-local and shift-invariant structures inherent in natural images.

Building upon the success of CSC, Pappayan et al. [11] further proposed the Multilayer Convolutional Sparse Coding (ML-CSC) problem in 2017. In the ML-CSC framework, the dictionary \mathbf{D} is modeled as a composition of several convolutional operators, enabling the encoding of progressively more complex features at multiple layers of abstraction.

Definition 1.1 (ML-CSC problem). *For a global observation signal \mathbf{y} , a set of convolutional dictionaries $\{\mathbf{D}_j\}_{j=1}^J$, and a vector $\boldsymbol{\lambda} \in \mathbb{R}_+^J$, define the deep convolutional sparse coding problem ($DCSC_\lambda$) as:*

$$\begin{aligned} (ML-CSC_\lambda) \quad \text{find} \quad \{\mathbf{x}_j\}_{j=1}^J \quad \text{s.t.} \quad & \mathbf{y} = \mathbf{D}_1\mathbf{x}_1, \quad \|\mathbf{x}_1\|_{0,\infty}^s \leq \lambda_1 \\ & \mathbf{x}_1 = \mathbf{D}_2\mathbf{x}_2, \quad \|\mathbf{x}_2\|_{0,\infty}^s \leq \lambda_2 \\ & \vdots \\ & \mathbf{x}_{J-1} = \mathbf{D}_J\mathbf{x}_J, \quad \|\mathbf{x}_J\|_{0,\infty}^s \leq \lambda_J, \end{aligned}$$

where λ_j is the j -th entry of the vector $\boldsymbol{\lambda}$ and $\|\mathbf{x}_j\|_{0,\infty}^s$ evaluates the maximum nonzero entries of stripe vectors of \mathbf{x}_j . $\|\cdot\|_{0,\infty}^s$ is specifically defined in [11] to measure local sparsity.

Pappayan et al. [11] also considered ML-CSC model with noise, changing constraints to be $\|\mathbf{y} - \mathbf{D}_1\mathbf{x}_1\|_2 \leq \varepsilon_1$ and $\|\mathbf{x}_j - \mathbf{D}_{j+1}\mathbf{x}_{j+1}\|_2 \leq \varepsilon_{j+1}$. Moreover, Pappayan et al. [11] made significant contributions to the theoretical understanding of sparse representations in the deep convolutional setting. They established precise recovery conditions for the sparse codes, demonstrating that the iterative thresholding algorithm used for optimization is intimately connected to the core mechanisms of convolutional neural networks (CNNs). This work provided a strong theoretical foundation for analyzing the sparse coding properties of deep learning architectures.

Under this framework, Sulam et al. [17] adopted a principled projection-based approach and a sound pursuit algorithm for solving the ML-CSC problem. Their work not only advanced the practical implementation of ML-CSC, but also developed tighter theoretical bounds on the recovery performance of the corresponding algorithms. Addressing an even more general model, Aberdam et al. [1] revealed deep connections with fully connected neural networks. Their analysis established stronger uniqueness guarantees and tighter bounds for oracle estimators, further solidifying the theoretical understanding of the ML-CSC framework. To simplify the complex optimization problem in deep pursuit, Sulam et al. [16] introduced an assumption that the intermediate layers are not perturbed. This allowed them to consider sparse penalties in a single optimization problem, rather than a layer-by-layer approach. They proposed the

ML-ISTA and ML-FISTA algorithms to efficiently solve this convex relaxation, and proved their convergence in terms of function value evaluations. Inspired by these developments, Rey et al. [12] explored additional convex alternatives and corresponding algorithms for the ML-CSC problem. Furthermore, Res-CSC and MSD-CSC [22], two variants of the ML-CSC model, were introduced to better understand the mechanisms of residual neural networks and mixed-scale dense neural networks, respectively.

Convolutional sparse coding (CSC) and its multi-layer extension, multi-layer CSC (ML-CSC), are powerful frameworks that leverage the convolutional structure of the dictionary \mathbf{D} to enable efficient and effective sparse representations. In these models, the dictionary \mathbf{D} is restricted to a convolutional form, and the activation function involved in the related neural networks is typically the rectified linear unit (ReLU), defined as $\sigma(x) = \max\{x, 0\}$.

In this work, we go beyond the standard CSC and ML-CSC formulations and develop a more general sparse coding model. We establish the uniqueness and stability properties of the sparse representations in this generalized framework, providing a strong theoretical foundation for the sparse coding problem. Building on these insights, we then explore the deep connection between our general sparse coding approach and the inner workings of convolutional neural networks (CNNs). We demonstrate that CNNs possess a remarkable capability in extracting sparse features, which can be viewed as a manifestation of the sparse coding principles. Inspired by these theoretical insights, we design a feature sparsity training strategy and compare the resulting performance and features in numerical experiments. Combining the theoretical and empirical findings with advanced approximation techniques, we further investigate the behavior of neural networks equipped with a wider range of activation functions and architectural designs. Specifically, the Deep Sparse Coding (DSC) problem under our consideration is given as follows.

Definition 1.2 (Deep sparse coding problem). *For a global noised signal \mathbf{y} , a set of dictionaries $\{\mathbf{D}_j\}_{j=1}^J$, a vector $\boldsymbol{\lambda} \in \mathbb{R}_+^J$, and a tolerance vector $\boldsymbol{\varepsilon} \in \mathbb{R}_+^J$, we call $\{\mathbf{x}_j\}_{j=1}^J$ a set of sparse codings of $DSC_{0,\boldsymbol{\lambda}}^\boldsymbol{\varepsilon}$ if it satisfies*

$$DSC_{0,\boldsymbol{\lambda}}^\boldsymbol{\varepsilon}(\mathbf{y}, \{\mathbf{D}_j\}_{j=1}^J) \quad \text{find} \quad \{\mathbf{x}_j\}_{j=1}^J \quad \text{s.t.} \quad \begin{aligned} \|\mathbf{y} - \mathbf{D}_1\mathbf{x}_1\|_2 &\leq \varepsilon_1, & \|\mathbf{x}_1\|_0 &\leq \lambda_1, \\ \|\mathbf{x}_1 - \mathbf{D}_2\mathbf{x}_2\|_2 &\leq \varepsilon_2, & \|\mathbf{x}_2\|_0 &\leq \lambda_2, \\ &\vdots \\ \|\mathbf{x}_{J-1} - \mathbf{D}_J\mathbf{x}_J\|_2 &\leq \varepsilon_J, & \|\mathbf{x}_J\|_0 &\leq \lambda_J. \end{aligned}$$

If we solve all feasible sets of sparse codings $\{\mathbf{x}_j\}_{j=1}^J$ under the constraint that $\boldsymbol{\varepsilon} = \mathbf{0}$, then we denote $DSC_{0,\boldsymbol{\lambda}}^\boldsymbol{\varepsilon} := DSC_{0,\boldsymbol{\lambda}}^0$. We call \mathbf{y} satisfies $DSC_{0,\boldsymbol{\lambda}}^\boldsymbol{\varepsilon}$ problem if there exists at least one set of feasible sparse coding.

It extends the Multilayer Convolutional Sparse Coding (ML-CSC) models by introducing more flexible dictionaries \mathbf{D}_j . The motivation behind these extensions stems from the practical observation that in image-related applications, different layers of neural networks extract feature representations at varying levels of abstraction. As one traverses the depth of a deep neural network, the learned features progress from low-level patterns, such as edges and textures, to higher-level semantic concepts and object-centric representations. This hierarchical and multi-scale nature of feature extraction is a hallmark of the success of deep learning in computer vision and other domains. By incorporating more flexible dictionaries and error tolerance, the Deep Sparse Coding (DSC) problem formulation aims to better capture this rich, multi-scale structure of feature representations. The increased flexibility allows the DSC model to adapt to the diverse characteristics of features at different network layers, rather than being constrained by the more rigid assumptions of the standard ML-CSC approach. Additionally, the error tolerance in the linear systems acknowledges the inherent approximations and imperfections that can arise when modeling the complex nonlinear transformations performed by deep neural architectures.

Contributions. we summarize several key contributions to the field of deep sparse feature extraction by deep neural networks:

- **Proposed DSC Models:** We introduce a novel class of Deep Sparse Coding (DSC) models and establish thorough theoretical analysis of their uniqueness and stability properties.
- **Convergence Rates via CNNs:** By applying iterative algorithms to the DSC models, we derive convergence rates for convolutional neural networks (CNNs) in their ability to extract sparse features. This provides a strong theoretical foundation for the use of CNNs in sparse feature learning tasks.
- **Extension to General Neural Networks:** The main result of our work is the extension of the convergence analysis to more general neural network architectures, including those with diverse activation functions, as well as self-attention and transformer-based models. This broadens the applicability of our findings to a wide range of deep learning methods for deep sparse feature extraction.
- **Encouraging Sparse Feature Learning:** Inspired by the strong connection between sparse coding and CNNs, we explore training strategies to encourage neural networks to learn more sparse features. We conduct numerical

experiments to evaluate the effectiveness of these approaches, providing valuable insights for the design of efficient deep learning algorithms.

2 Uniqueness and stability of the deep sparse feature model

One central challenge that arises when we translate from the (P_0) problem to the relaxed versions, (P_0^ε) or $(P_{1,\lambda})$, is assessing the effectiveness of these solutions in recovering the sparse coding problem, (P_0) . One frequently employed metric for this evaluation in the large literature of compressed sensing is the mutual coherence, which is also important in the following discussion.

Definition 2.1. Denote the k -th column of $\mathbf{A} \in \mathbb{R}^{m \times d}$ by \mathbf{a}_k . Then the mutual-coherence of the matrix \mathbf{A} is given by

$$\mu(\mathbf{A}) = \max_{i \neq j} \frac{|\mathbf{a}_i^\top \mathbf{a}_j|}{\|\mathbf{a}_i\|_2 \|\mathbf{a}_j\|_2}.$$

The first important question is whether there exists a unique solution to $(DSC_{0,\lambda}^0)$ problem. The following result characterizes the required conditions.

Theorem 2.1 (Uniqueness via mutual coherence without noise). *Given a set of dictionaries $\{\mathbf{D}_j\}_{j=1}^J$ and consider a signal \mathbf{y} , satisfying the $(DSC_{0,\lambda}^0)$ problem, and assume that $\{\mathbf{x}_j\}_{j=1}^J$ is a solution to $(DSC_{0,\lambda}^0)$. If for any j ,*

$$\|\mathbf{x}_j\|_0 < \frac{1}{2} \left(1 + \frac{1}{\mu(\mathbf{D}_j)} \right),$$

then $\{\mathbf{x}_j\}_{j=1}^\infty$ is the unique solution to the $(DCP_{0,\lambda}^0)$ problem with

$$\lambda_j < \frac{1}{2} \left(1 + \frac{1}{\mu(\mathbf{D}_j)} \right).$$

Proof. Theorem 2.5 in [5] asserts that if $\mathbf{y} = \mathbf{D}_1 \mathbf{x}_1$ has a solution satisfying $\|\mathbf{x}_1\|_0 < \frac{1}{2} \left(1 + \frac{1}{\mu(\mathbf{D}_1)} \right)$, then \mathbf{x}_1 is the unique and sparsest solution. Together with the condition $\lambda_1 < \frac{1}{2} \left(1 + \frac{1}{\mu(\mathbf{D}_1)} \right)$, we conclude that \mathbf{x}_1 is unique. Similarly and iteratively, the conditions guarantee that \mathbf{x}_j is unique for $j = 2, \dots, J$, which leads to the result. \square

Notice that Definition 1.2 and Theorem 2.1 are similar to Definition 1.1 in [11]. However, the conditions here are weaker since the dictionaries in [11] are assumed to be convolutional ones. There exist two ways to further relax the condition for the uniqueness, introduced in [1, 17]. Noticing that for $(DSC_{0,\lambda}^0)$, we have $\mathbf{y} = \mathbf{D}_1 \cdots \mathbf{D}_j \mathbf{x}_j$ and $\mathbf{x}_j = \mathbf{D}_{j+1} \cdots \mathbf{D}_{j+m} \mathbf{x}_{j+m}$. Denoting $\mathbf{D}_{[j]} := \mathbf{D}_1 \cdots \mathbf{D}_j$ and $\mathbf{D}_{[j,j+m]} := \mathbf{D}_j \cdots \mathbf{D}_{j+m}$, it is easy to see that for the uniqueness of a sparse coding \mathbf{x}_{j_0} from layer j_0 , we can consider the solutions of $\mathbf{y} = \mathbf{D}_{[j_0]} \mathbf{x}_{j_0}$ or $\mathbf{x}_j = \mathbf{D}_{[j,j_0]} \mathbf{x}_{j_0}$ for any $j < j_0$ if \mathbf{x}_j is unique. It implies that if the uniqueness of \mathbf{x}_j holds, together with the result in Theorem 2.1, we only need to require λ_{j_0} to be bounded as

$$\lambda_{j_0} < \frac{1}{2} \max \left\{ 1 + \frac{1}{\mu(\mathbf{D}_{[j_0]})}, 1 + \frac{1}{\mu(\mathbf{D}_{[j_0]})}, 1 + \frac{1}{\mu(\mathbf{D}_{[j,j_0]})} : j < j_0 \right\}, \quad (1)$$

then we can make sure \mathbf{x}_{j_0} is unique for $(DSC_{0,\lambda}^0)$.

The above approach is a top-bottom layer-by-layer approach. Let us think about extracting sparse codings simultaneously and conversely. Assume that we know the support of each \mathbf{x}_j . We denote the support of \mathbf{x}_j as \mathcal{S}_j and collect its nonzero elements in $\mathbf{x}_{j,\mathcal{S}_j}$. Let $\mathbf{A}_{\mathcal{S}_i,\mathcal{S}_j}$ be the submatrix of matrix \mathbf{A} with the indices of rows from \mathcal{S}_i and columns from \mathcal{S}_j . Collecting nonzero elements of \mathbf{x}_j row-wise, then solving $(DSC_{0,\lambda}^0)$ is equivalent to solving the following linear system

$$\begin{pmatrix} \mathbf{x}_{1,\mathcal{S}_1^c} \\ \mathbf{x}_{2,\mathcal{S}_2^c} \\ \vdots \\ \mathbf{x}_{J-1,\mathcal{S}_{J-1}^c} \end{pmatrix} = \begin{pmatrix} (\mathbf{D}_{[2,J]})_{\mathcal{S}_1^c,\mathcal{S}_J} \\ (\mathbf{D}_{[3,J]})_{\mathcal{S}_2^c,\mathcal{S}_J} \\ \vdots \\ (\mathbf{D}_{[J,J]})_{\mathcal{S}_{J-1}^c,\mathcal{S}_J} \end{pmatrix} \mathbf{x}_{J,\mathcal{S}_J} =: \mathbf{D}^{[\mathcal{S}_J]} \mathbf{x}_{J,\mathcal{S}_J}. \quad (2)$$

Since the left-hand side of (2) is actually a zero vector, to get \mathbf{x}_{J,S_J} , we only need to search in the null space of $\mathbf{D}^{[S_J]}$, which is of dimension $\lambda_J - \text{rank}(\mathbf{D}^{[S_J]})$ and smaller than λ_J . After getting the deepest sparse coding, push back through the equation $\mathbf{x}_{j-1} = \mathbf{D}_j \mathbf{x}_j$, we completely solve $(DSC_{0,\lambda}^0)$. Although this idea helps to relax the conditions as well as the complexity, usually one does not know the supports of the underlying sparse features and hence the second method does not match well with general applications of interest. Refer to [1] for more details.

With the uniqueness condition, one may wonder whether we can solve this problem through some algorithms. Usually people relax ℓ_0 problems to ℓ_1 ones. Similarly we also establish the relationship between $(DSC_{0,\lambda}^0)$ and the following deep convex optimization problem (DSC_1) , which could be solved through convex optimization algorithms.

Definition 2.2 (DSC_1). For a global observation signal \mathbf{y} and a set of dictionaries $\{\mathbf{D}_j\}_{j=1}^J$, define the deep coding problem (DSC_1) as:

$$\begin{aligned} DSC_1(\mathbf{y}, \{\mathbf{D}_j\}_{j=1}^J) \quad \text{find} \quad \{x_j\}_{j=1}^J \quad \text{s.t.} \quad & \mathbf{x}_1 := \argmin \{\|\mathbf{x}\|_1 : \mathbf{y} = \mathbf{D}_1 \mathbf{x}\}, \\ & \mathbf{x}_2 := \argmin \{\|\mathbf{x}\|_1 : \mathbf{x}_1 = \mathbf{D}_2 \mathbf{x}\}, \\ & \vdots \\ & \mathbf{x}_J := \argmin \{\|\mathbf{x}\|_1 : \mathbf{x}_{J-1} = \mathbf{D}_J \mathbf{x}\}. \end{aligned}$$

The next theorem characterizes when the two problems have the same unique solution.

Theorem 2.2 (Coincidence between ℓ_0 and ℓ_1 problems). Let $\{\mathbf{D}_j\}_{j=1}^J$ be a set of dictionaries with each \mathbf{D}_j of full row rank. Assume that the conditions in Theorem 2.1 are satisfied and $\{\mathbf{x}_j\}_{j=1}^J$ is a solution of $DSC_{0,\lambda}^0$. Then $\{\mathbf{x}_j\}_{j=1}^J$ is the unique solution of $DSC_{0,\lambda}^0$ and DSC_1 .

Proof. Theorem 2.5 and Theorem 4.5 in [5] imply that if there exists a solution \mathbf{x}_1 of $\mathbf{y} = \mathbf{D}_1 \mathbf{x}_1$ such that $\|\mathbf{x}_1\|_0 \leq \frac{1}{2}(1 + \frac{1}{\mu(\mathbf{D}_1)})$, then \mathbf{x}_1 is unique and $\mathbf{x}_1 = \argmin \{\|\mathbf{x}\|_1 : \mathbf{y} = \mathbf{D}_1 \mathbf{x}\}$. Hence, iteratively we are able to show the statement. \square

Theorem 2.2 indicates that we have various methods to solve $(DSC_{0,\lambda}^0)$ by solving DSC_1 and convergence analysis can be done iteratively. In the next section, we shall construct CNNs that can solve $(DSC_{0,\lambda}^0)$ with exponential decay.

In real world problems, there usually exists noise which may occur during sampling or computing. How do the solutions change when noise occurs? Before considering the robustness of deep sparse coding, for simplicity of statements throughout this work, we shall introduce the following uniqueness condition.

Assumption 1 (Uniqueness condition). The parameters λ and \mathbf{D}_j of Definition 1.2 satisfy the following sparsity condition

$$\lambda_j < \frac{1}{2} \left(1 + \frac{1}{\mu(\mathbf{D}_j)} \right), \forall j \in [J].$$

Theorem 2.3 (Stability of $(DSC_{0,\lambda}^0)$ problem). Given a set of dictionaries $\{\mathbf{D}_j\}_{j=1}^J$ with each dictionary \mathbf{D}_j being column-normalized with respect to the ℓ_2 norm and the sparsity level λ satisfying Assumption 1. Let \mathbf{y} be a global observation that satisfies Definition 1.2 and $\tilde{\mathbf{y}}$ be a noised global observation $\tilde{\mathbf{y}} = \mathbf{y} + \varepsilon_0$ for some noise ε_0 . If the collections $\{\mathbf{x}_j\}_{j=1}^J$ and $\{\tilde{\mathbf{x}}_j\}_{j=1}^J$ are solutions to $DCP_{0,\lambda}^0(\mathbf{y}, \{\mathbf{D}_j\}_{j=1}^J)$ and $DCP_{0,\lambda}^\varepsilon(\tilde{\mathbf{y}}, \{\mathbf{D}_j\}_{j=1}^J)$, respectively, then they must obey

$$\|\mathbf{x}_j - \tilde{\mathbf{x}}_j\|_2^2 \leq \delta_j^2$$

where δ_j is defined as

$$\begin{aligned} \delta_0 &= \|\varepsilon_0\|_2, \\ \delta_j &= \frac{\varepsilon_j + \delta_{j-1}}{\sqrt{1 - (2\lambda_j - 1)\mu(\mathbf{D}_j)}}, \quad j = 1, 2, \dots, J. \end{aligned}$$

Proof. The proof is partially inspired by Section 5.2.3 of [5]. Let $\mathbf{Q} = \mathbf{1}\mathbf{1}^\top$ with the constant 1 vector $\mathbf{1}$. Then it is easy to see that for any \mathbf{x} with sparsity $\|\mathbf{x}\|_0 \leq s$,

$$\begin{aligned} \|\mathbf{D}\mathbf{x}\|_2^2 &= \mathbf{x}^\top \mathbf{D}^\top \mathbf{D} \mathbf{x} \geq \mathbf{x}^\top \mathbf{x} + \mu(\mathbf{D})|\mathbf{x}|^\top (\mathbf{I} - \mathbf{Q})|\mathbf{x}| \\ &\geq (1 + \mu(\mathbf{D})) \|\mathbf{x}\|_2^2 - \mu(\mathbf{D}) \|\mathbf{x}\|_1^2 \\ &\geq (1 + \mu(\mathbf{D})) \|\mathbf{x}\|_2^2 - \mu(\mathbf{D}) s \|\mathbf{x}\|_2^2 \\ &= (1 - (s - 1)\mu(\mathbf{D})) \|\mathbf{x}\|_2^2, \end{aligned} \tag{3}$$

where in the third step we use the inequality $\|\mathbf{c}\|_1 \leq \sqrt{s}\|\mathbf{c}\|_2$ for any $\mathbf{c} \in \mathbb{R}^s$ and in the first step, with $|\mathbf{x}| := (|x_i|) \in \mathbb{R}^m$, we use the following fact

$$\mathbf{x}^\top \mathbf{D}^\top \mathbf{D} \mathbf{x} = \|\mathbf{x}\|_2^2 + \sum_{i \neq j} \mathbf{d}_i^\top \mathbf{d}_j x_i x_j \geq \|\mathbf{x}\|_2^2 - \sum_{i \neq j} \mu(\mathbf{D}) |x_i x_j| = \|\mathbf{x}\|_2^2 - \mu(\mathbf{D}) |\mathbf{x}|^\top (\mathbf{Q} - \mathbf{I}) |\mathbf{x}|.$$

Since $\mathbf{y} = \mathbf{D}_1 \mathbf{x}_1$, $\|\tilde{\mathbf{y}} - \mathbf{D}_1 \tilde{\mathbf{x}}_1\|_2 \leq \varepsilon_1$, and $\|\mathbf{y} - \tilde{\mathbf{y}}\|_2 = \|\varepsilon_0\|_2$, we have $\|\mathbf{D}_1 \mathbf{x}_1 - \mathbf{D}_1 \tilde{\mathbf{x}}_1\|_2 \leq \|\varepsilon_0\|_2 + \varepsilon_1$. Combining this with (3) and $\|\mathbf{x}_1 - \tilde{\mathbf{x}}_1\|_0 \leq 2\lambda_1$, we have

$$\|\mathbf{x}_1 - \tilde{\mathbf{x}}_1\|_2^2 \leq \frac{(\|\varepsilon_0\|_2 + \varepsilon_1)^2}{1 - (2\lambda_1 - 1)\mu(\mathbf{D}_1)}. \quad (4)$$

Again, combining $\|\tilde{\mathbf{x}}_1 - \mathbf{D}_2 \tilde{\mathbf{x}}_2\|_2 \leq \varepsilon_2$, $\mathbf{x}_1 = \mathbf{D}_2 \mathbf{x}_2$, and (4), we obtain

$$\|\mathbf{D}_2 \mathbf{x}_2 - \mathbf{D}_2 \tilde{\mathbf{x}}_2\|_2 \leq \varepsilon_2 + \frac{\|\varepsilon_0\|_2 + \varepsilon_1}{\sqrt{1 - (2\lambda_1 - 1)\mu(\mathbf{D}_1)}}. \quad (5)$$

Denote

$$\delta_1 := \frac{\|\varepsilon_0\|_2 + \varepsilon_1}{\sqrt{1 - (2\lambda_1 - 1)\mu(\mathbf{D}_1)}}.$$

Consequently, by (3) and (5), we have

$$\|\mathbf{x}_2 - \tilde{\mathbf{x}}_2\|_2^2 \leq \frac{(\varepsilon_2 + \delta_1)^2}{1 - (2\lambda_2 - 1)\mu(\mathbf{D}_2)},$$

Repeating the above step for j from 3 to J , we conclude that

$$\|\mathbf{x}_j - \tilde{\mathbf{x}}_j\|_2^2 \leq \frac{(\varepsilon_j + \delta_{j-1})^2}{1 - (2\lambda_j - 1)\mu(\mathbf{D}_j)},$$

with δ_j defined iteratively as in the statements. □

The following two corollaries give a clearer representation, showing that in the noise case, solutions are not far from the unique solution, with the distance being bounded in order by noise levels.

Corollary 2.4. Assume that the conditions of Theorem 2.3 hold and $\varepsilon_j = 0$, $j = 1, \dots, J$. If the collections $\{\mathbf{x}_j\}_{j=1}^J$ and $\{\tilde{\mathbf{x}}_j\}_{j=1}^J$ satisfy $DCP_{0,\lambda}^0(\mathbf{y}, \{\mathbf{D}_j\}_{j=1}^J)$ and $DCP_{0,\lambda}^0(\tilde{\mathbf{y}}, \{\mathbf{D}_j\}_{j=1}^J)$, respectively, then they must obey

$$\|\tilde{\mathbf{x}}_j - \mathbf{x}_j\|_2^2 \leq \|\varepsilon_0\|_2^2 \left(\prod_{i=1}^j (1 - (2\lambda_i - 1)\mu(\mathbf{D}_i)) \right)^{-1}.$$

Corollary 2.5. Assume that the conditions of Theorem 2.3 hold and $\varepsilon_0 = 0$. If the collections $\{\mathbf{x}_j\}_{j=1}^J$ and $\{\tilde{\mathbf{x}}_j\}_{j=1}^J$ satisfy $DCP_{0,\lambda}^0(\mathbf{y}, \{\mathbf{D}_j\}_{j=1}^J)$ and $DCP_{0,\lambda}^\varepsilon(\mathbf{y}, \{\mathbf{D}_j\}_{j=1}^J)$, respectively, then they must obey

$$\|\tilde{\mathbf{x}}_j - \mathbf{x}_j\|_2 \leq \frac{\sum_{i=1}^j \varepsilon_i \prod_{k=1}^{i-1} \sqrt{1 - (2\lambda_k - 1)\mu(\mathbf{D}_k)}}{\prod_{i=1}^j \sqrt{1 - (2\lambda_i - 1)\mu(\mathbf{D}_i)}}.$$

As pointed out in [11], results for convolutional dictionaries can be applied to general dictionaries by viewing convolution kernel having the same size as the column of dictionaries (in this way their results do not work for convolutional neural networks). However, in [11, 1], they consider the same case as Corollary 2.4 and the obtained upper bound is

$$4\|\varepsilon_0\|_2^2 \left(\prod_{i=1}^j (1 - (2\lambda_i - 1)\mu(\mathbf{D}_i)) \right)^{-1}$$

In [17], models in Corollary 2.5 are discussed and the obtained upper bound is

$$4\|\varepsilon_0\|_2^2 \left(\prod_{i=1}^j 4^{1-i} (1 - (2\lambda_i - 1)\mu(\mathbf{D}_i)) \right)^{-1}.$$

Hence our bound is tighter for general dictionaries.

The above stability analysis is based on a layer-by-layer approach. Using the idea discussed for (1), One can generalize the conclusion of Theorem 2.3 to

$$\|\tilde{\mathbf{x}}_{j_0} - \mathbf{x}_{j_0}\|_2^2 \leq \frac{(\varepsilon_{[j,j_0]} + \delta_j)^2}{1 - (2\lambda_j - 1)\mu(\mathbf{D}_{[j,j_0]})}, \quad j < j_0$$

when we already have the noise information of layer j and j_0 , i.e., $\|\mathbf{x}_j - \tilde{\mathbf{x}}_j\|_2^2 \leq \delta_j^2$ and $\|\tilde{\mathbf{x}}_j - \mathbf{D}_{[j,j_0]}\tilde{\mathbf{x}}_{j_0}\|_2 \leq \varepsilon_{[j,j_0]}$, respectively. In this way, the obtained error bound does not need to cumulate from j -th layer to j_0 -th layer. If one wishes to consider all sparse codings as (2) in a single equation, i.e., we directly use the deepest information $\|\mathbf{D}^{[S_J]}\mathbf{x}_{J,S_J} - \mathbf{D}^{[S_J]}\tilde{\mathbf{x}}_{J,S_J}\|_2 \leq \varepsilon$, then the problem is reduced to a shallow case (i.e., $J = 1$) and with (3), we immediately obtain

$$\|\mathbf{x}_{J,S_J} - \tilde{\mathbf{x}}_{J,S_J}\|_2 \leq \varepsilon \left(1 - (2\lambda_J - 1)\mu(\mathbf{D}^{[S_J]})\right)^{-1/2}.$$

When setting

$$\tilde{\mathbf{x}}_{j,S_j} := (\mathbf{D}_{[j,J]})_{S_j,S_J} \tilde{\mathbf{x}}_{J,S_J},$$

the layer- j error is given by

$$\|\mathbf{x}_{j,S_j} - \tilde{\mathbf{x}}_{j,S_j}\|_2 \leq \varepsilon \left\| (\mathbf{D}_{[j,J]})_{S_j,S_J} \right\|_2 \left(1 - (2\lambda_J - 1)\mu(\mathbf{D}^{[S_J]})\right)^{-1/2},$$

which also yields a non-cumulative bound. The above discussion suggests that in applications, conditions required could be more optimistic than those required in Theorem 2.3.

In the following, to deepen the CNNs in Definition 3.1 below, when features of the output of each channel from some layers are of dimension one, we regard them as vectors with only one channel. In this way, CNNs can have an arbitrary depth, which enables better learning abilities.

3 Deep sparse feature extraction via deep convolutional neural networks

CNNs studied in this paper have multiple channels because the convolution we use does not allow zero-padding, and the widths decreases as the layers. When zero-padding convolutions are used, the CNNs can have good learning abilities even with one channel [23, 24, 8].

Let s, t, d be integers. Here and below we set $\mathcal{D}(d, t) := \lceil d/t \rceil$ the smallest integer no less than d/t and $A_{i,j}$ the (i, j) th entry of a matrix $\mathbf{A} \in \mathbb{R}^{m \times n}$ with $A_{i,j} = 0$ if $i \notin [1, m]$ or $j \notin [1, n]$. We shall use $\mathbf{1}_{m \times n} := (\mathbf{1})_{i \in [m], j \in [n]}$ to represent constant 1 matrix of dimension $m \times n$. Similar setting works for vectors. Denote \mathcal{T}_α the soft thresholding function defined componentwise as

$$\mathcal{T}_\alpha(\mathbf{x})_i = \text{sign}(x_i)(|x_i| - \alpha)_+.$$

In the following, we shall simply denote the result of soft thresholding as $\mathcal{T}_\alpha(\mathbf{x})$.

3.1 Convolutional neural networks

The 1-D convolution of size s , stride t is computed for a kernel $\mathbf{w} \in \mathbb{R}^s$ and a digital signal $\mathbf{x} \in \mathbb{R}^d$ to be $\mathbf{w} *_t \mathbf{x} \in \mathbb{R}^{\mathcal{D}(d,t)}$ by

$$(\mathbf{w} *_t \mathbf{x})_i = \sum_{k=1}^s w_k x_{(i-1)t+k}, \quad i = 1, \dots, \mathcal{D}(d, t).$$

A multi-channel DCNN consists of more than 1 convolutional layers and multiple channels in each layer and is defined as follows.

Definition 3.1. Given the input size $d \in \mathbb{N}$, a multi-channel DCNN in 1D of depth J with respect to filter size $\{s_j \geq 2\}_{j=1}^J$, stride $\{t_j \geq 1\}_{j=1}^J$ and channel $\{n_j \geq 1\}_{j=1}^J$, is a neural network $\{h_j : \mathbb{R}^d \rightarrow \mathbb{R}^{d_j \times n_j}\}_{j=1}^J$ defined iteratively for which $h_0(\mathbf{x}) = \mathbf{x} \in \mathbb{R}^d$, $d_0 = d$, $n_0 = 1$, and the ℓ -th channel of h_j is given by

$$h_j(\mathbf{x})_\ell = \sigma \left(\sum_{i=1}^{n_{j-1}} \mathbf{w}_{\ell,i}^{(j)} *_t h_{j-1}(\mathbf{x})_i + b_\ell^{(j)} \mathbf{1}_{d_j} \right),$$

for $j = 1, \dots, J$, $\ell = 1, \dots, n_j$, where $b_\ell^{(j)} \in \mathbb{R}$ are biases, $\mathbf{w}_{\ell,i}^{(j)} \in \mathbb{R}^{s_j}$ are filters, $d_j = \mathcal{D}(d_{j-1}, t_j)$, and $\sigma(u) = \max\{u, 0\}$, $u \in \mathbb{R}$ is the rectified linear unit (ReLU) activation.

The vast majority of DCNNs in practical applications of deep learning in image processing are induced by 2-D convolutions. As an analogy of the 1-D case, 2-D convolutions and DCNNs can be well defined. Precisely, here the 2-D convolution of a filter $\mathbf{W} \in \mathbb{R}^{s \times s}$ and a digital image $\mathbf{X} \in \mathbb{R}^{d \times d}$ with stride t produce a convoluted matrix $\mathbf{W} \circledast_t \mathbf{X} \in \mathbb{R}^{\mathcal{D}(d,t) \times \mathcal{D}(d,t)}$ for which the (i, j) -entry is given by

$$(\mathbf{W} \circledast_t \mathbf{X})_{(i,j)} := \sum_{\ell_1, \ell_2=1}^s W_{\ell_1, \ell_2} X_{(i-1)t+\ell_1, (j-1)t+\ell_2}, \quad i, j = 1, \dots, \mathcal{D}(d, t).$$

Definition 3.2. Given input signal $\mathbf{X} \in \mathbb{R}^{d \times d}$, a multi-channel DCNN in 2D of depth J with respect to filter size $s_j \geq 2$, stride $t_j \geq 1$ and channel $n_j \geq 1$, $j = 1, \dots, J$ is a neural network $\{h_j : \mathbb{R}^{d \times d} \rightarrow \mathbb{R}^{d_j \times d_j \times n_j}\}_{j=1}^J$ defined iteratively for which $h_0(\mathbf{X}) = \mathbf{X} \in \mathbb{R}^{d \times d}$, $d_0 = d$, $n_0 = 1$, and the ℓ th channel of h_j is given by

$$h_j(\mathbf{X})_\ell = \sigma \left(\sum_{i=1}^{n_{j-1}} \mathbf{W}_{\ell, i}^{(j)} \circledast_{t_j} h_{j-1}(\mathbf{X})_i + B_\ell^{(j)} \mathbf{1}_{d_j \times d_j} \right),$$

for $j = 1, \dots, J$, $\ell = 1, \dots, n_j$, where $\mathbf{W}_{\ell, i}^{(j)} \in \mathbb{R}^{s_j \times s_j}$ are filters, $B_\ell^{(j)} \in \mathbb{R}$ are bias, and $d_j = \mathcal{D}(d_{j-1}, t_j)$.

In this work, we concentrate on the outcomes associated with deep sparse coding through the use of 1-D DCNNs. Notably, the results we present here can be readily extended to 2-D DCNNs and hence offer potential insights into a broader range of applications. When outputs of convolutional layers have dimension 1 in each channel, we simply flatten them to be vectors without additional notations for simplicity and hence naturally they can be viewed as inputs of other convolutional neural networks.

To establish convergence rates for approximating sparse codings with noise, we need the ground truth sparse codings and noise to be bounded.

Assumption 2. The signal \mathbf{x}^* and the observation noise $\boldsymbol{\varepsilon}$ are assumed to be bounded

$$(\mathbf{x}^*, \boldsymbol{\varepsilon}) \in \mathbb{X}(B, \delta) := \{(\mathbf{x}^*, \boldsymbol{\varepsilon}) : |\mathbf{x}_i^*| \leq B, \forall i, \|\boldsymbol{\varepsilon}\|_1 \leq \delta\}.$$

Next, we shall use the convergence of LISTA-CP [2] to conduct feature approximation analysis for deep sparse coding problems.

Theorem 3.1 (Exponential convergence w.r.t. ℓ_2 norm). Given a set of dictionaries $\{\mathbf{D}_j \in \mathbb{R}^{d_{j-1} \times d_j}\}_{j=1}^J$ with each dictionary \mathbf{D}_j being column-normalized with respect to the ℓ_2 norm. We assume that the global observation \mathbf{y} satisfies Definition 1.2 and each \mathbf{x}_j in the corresponding solution $\{\mathbf{x}_j\}_{j=1}^J$ satisfies Assumption 1 and Assumption 2, i.e. $\|\mathbf{x}_j\|_0 \leq \lambda_j$ and $(\mathbf{x}_j, \boldsymbol{\varepsilon}_j) \in \mathbb{X}(B_j, \delta_j)$. Then there exists a CNN with kernel size s , depth $O(K \log_s \prod_{j=1}^J (d_{j-1} + d_j))$ and number of weights $O(K \prod_{j=1}^J (d_{j-1} + d_j)^2)$ such that the output, denoted by $\{\tilde{\mathbf{x}}_j\}_{j=1}^J$, satisfies

$$\|\tilde{\mathbf{x}}_j - \mathbf{x}_j\|_2 \leq C_{\mathbf{D}, \mathbf{B}, \boldsymbol{\lambda}} e^{-c_{\mathbf{D}, \boldsymbol{\lambda}} K} + C_{\mathbf{D}} \sum_{i=1}^j \delta_i.$$

where $c_{\mathbf{D}, \boldsymbol{\lambda}}, C_{\mathbf{D}}, C_{\mathbf{D}, \mathbf{B}, \boldsymbol{\lambda}} > 0$ denote constants depending only on $\{\mathbf{D}_j\}_{j=1}^J$, $\boldsymbol{\lambda}$ and $\mathbf{B} := \{B_j\}_{j=1}^J$.

The proof can be found in Appendix 1. Recall that when deep sparse coding is noiseless, Theorem 2.2 indicates there exists an algorithm that can find the unique solution. We shall show that the unique solution can be achieved by CNNs with depth only increasing as fast as $O(|\log_2 \varepsilon|)$ for some given error tolerance ε .

Corollary 3.2 (Deep sparse coding without noise). Under the assumptions and conditions of Theorem 3.1 with $\boldsymbol{\varepsilon}_j = 0$ and $B_j \leq B$, $j = 1, \dots, J$, there exists a CNN with kernel size s , depth $O(K \log_s \prod_{j=1}^J (d_{j-1} + d_j))$ and number of weights $O(K \prod_{j=1}^J (d_{j-1} + d_j)^2)$ such that the output $\{\tilde{\mathbf{x}}_j\}_{j=1}^J$ satisfies

$$\|\tilde{\mathbf{x}}_j - \mathbf{x}_j\|_2 = O(C_{\mathbf{D}, \mathbf{B}, \boldsymbol{\lambda}} e^{-c_{\mathbf{D}, \boldsymbol{\lambda}} K}).$$

In other words, a CNN with depth $O(|\log_2 \varepsilon|)$ can approximate sparse codings with error ε .

We can also generalize our results to the ℓ_2 - ℓ_1 loss.

Corollary 3.3 (Exponential convergence w.r.t. ℓ_2 - ℓ_1 loss). *Given $\gamma > 0$, denote the ℓ_2 - ℓ_1 loss as $L_j(\mathbf{x}) = \|\mathbf{x}_{j-1} - \mathbf{D}_j \mathbf{x}\|_2^2 + \gamma \|\mathbf{x}\|_1$ for $\{\mathbf{x}_j\}_{j=1}^J$ and $\mathbf{x}_0 := \mathbf{y}$. Under the conditions of Corollary 3.2, there exists a CNN with kernel size s , depth $O\left(K \log_s \prod_{j=1}^J (d_{j-1} + d_j)\right)$ and number of weights $O\left(K \prod_{j=1}^J (d_{j-1} + d_j)^2\right)$ such that the output $\{\tilde{\mathbf{x}}_j\}_{j=1}^J$ satisfies*

$$0 \leq L_j(\tilde{\mathbf{x}}_j) - L_j(\mathbf{x}_j) \leq C_{\mathbf{D}, \mathbf{B}, \lambda} e^{-c_{\mathbf{D}, \lambda} K}.$$

Proof. Since \mathbf{x}_j is the unique solution of the sparse linear inverse problem $\mathbf{x}_{j-1} = \mathbf{D}_j \mathbf{x}$ with smallest ℓ_1 norm requirement of solution \mathbf{x} , we have $L_j(\mathbf{x}) - L_j(\mathbf{x}_j) \geq 0$ for any \mathbf{x} and $L_j(\mathbf{x}_j) = \gamma \|\mathbf{x}_j\|_1$. Then

$$\begin{aligned} L_j(\tilde{\mathbf{x}}_j) - L_j(\mathbf{x}_j) &\leq \|\mathbf{x}_{j-1} - \mathbf{D}_j \tilde{\mathbf{x}}_j\|_2^2 + \gamma (\|\tilde{\mathbf{x}}_j\|_1 - \|\mathbf{x}_j\|_1) \\ &\leq \|\mathbf{D}_j \mathbf{x}_j - \mathbf{D}_j \tilde{\mathbf{x}}_j\|_2^2 + \gamma (\|\tilde{\mathbf{x}}_j - \mathbf{x}_j\|_1) \\ &\leq \|\mathbf{D}_j\|_2^2 \|\mathbf{x}_j - \tilde{\mathbf{x}}_j\|_2^2 + \gamma \sqrt{\lambda_j} \|\tilde{\mathbf{x}}_j - \mathbf{x}_j\|_2 \\ &\leq B^2 \|\mathbf{D}_j\|_2^2 e^{-2cK} \left(\sum_{i=1}^j \lambda_i \right)^2 + \gamma \sqrt{\lambda_j} B e^{-cK} \sum_{i=1}^j \lambda_i \\ &\leq C \gamma \sqrt{\lambda_j} B^2 \|\mathbf{D}_j\|_2^2 e^{-cK} \left(\sum_{i=1}^j \lambda_i \right)^2, \end{aligned}$$

where we used the fact $\|\mathbf{c}\|_1 \leq \sqrt{s} \|\mathbf{c}\|_2$ for any $\mathbf{c} \in \mathbb{R}^s$ and $\tilde{\mathbf{x}}_j$ successfully recovered the support of \mathbf{x}_j . The proof is completed. \square

It is also worth to extend our result to CNNs activated by general ReLU type activation functions, which include LeakyReLU and ELU. Let $\rho \in C((-\infty, \infty))$ be a generalized ReLU type activation function, which takes the value x for $x \geq 0$ and $|\rho(x)| \leq \beta$ for $x < 0$ with some $\beta \geq 0$. Furthermore, we assume that ρ is Lipschitz with constant L , i.e. $|\rho(x) - \rho(y)| \leq L|x - y|$.

Theorem 3.4. *Let $m \in \mathbb{N}_+$. Given a set of dictionaries $\{\mathbf{D}_j \in \mathbb{R}^{d_{j-1} \times d_j}\}_{j=1}^J$ with each dictionary \mathbf{D}_j being column-wisely normalized with respect to the ℓ_2 norm. We assume that the global observation \mathbf{y} satisfies Definition 1.2 and each \mathbf{x}_j in the corresponding solution $\{\mathbf{x}_j\}_{j=1}^J$ satisfies Assumption 1, Assumption 2 and $\lambda_j < \frac{1}{2-2L^m} \left(\frac{1}{\mu} - 2L^m d \right)$.*

Then there exists a CNN activated by ρ with kernel size s , depth $O\left(mK \log_s \prod_{j=1}^J (d_{j-1} + d_j)\right)$ and number of weights $O\left(mK \prod_{j=1}^J (d_{j-1} + d_j)^2\right)$ such that the output $\{\tilde{\mathbf{x}}_j\}_{j=1}^J$ satisfies

$$\|\tilde{\mathbf{x}}_j - \mathbf{x}_j\|_2 \leq C_{\mathbf{D}, \mathbf{B}, \lambda} e^{-c_{\mathbf{D}, \lambda} K} + C_{\mathbf{D}, \mathbf{B}, \lambda} \sum_{i=1}^j \delta_i + C_{\mathbf{D}, \mathbf{B}, \lambda} \beta L^{m-1},$$

where $c_{\mathbf{D}, \lambda} > 0$ and $C_{\mathbf{D}, \mathbf{B}, \lambda} > 0$ only depend on $\{\mathbf{D}_j\}_{j=1}^J$, λ and $\mathbf{B} := \{B_j\}_{j=1}^J$.

For non-ReLU type activation functions, we can apply the following result.

Theorem 3.5. *Assume that there exists a neural network ϕ_ρ (with finite neurons) activated by ρ such that $\|\phi_\rho - \sigma\|_{L_\infty([-M, M])} = \varepsilon$ where ε depends on the depth/width/number of parameters of ϕ_ρ and M is large enough. Then under the conditions of Theorem 3.1, there exists a neural network Φ_ρ such that we can find its J intermediate outputs $\{\tilde{\mathbf{x}}_j\}_{j=1}^J$ such that*

$$\|\tilde{\mathbf{x}}_j - \mathbf{x}_j\|_2 \leq C_{\mathbf{D}, \mathbf{B}, \lambda} e^{-c_{\mathbf{D}, \lambda} K} + C_{\mathbf{D}, \mathbf{B}, \lambda} \sum_{i=1}^j \delta_i + C_{\mathbf{D}, \mathbf{B}, \lambda} \varepsilon.$$

Remark 3.6 (deep sparse coding via self attention and transformer). *Attention mechanism is a widely used technique in deep learning, originating from some phenomena that human beings awareness is likely to concentrate on important information. Scaled dot-product attention [18] contains three part: key \mathbf{K} , value \mathbf{V} , and query \mathbf{Q} , and they are linear transforms of input matrix \mathbf{X} . It is found that scaled dot-product attention together with positional encoding can approximate any convolutional neural networks [4]. Moreover, the truck of transformer can be briefly formulated as alternatively applying scaled dot-product attention and the fully connected neural networks [18]. Hence, combing results in [4], our results established in this section can be directly extended to scaled dot-product attention and transformer, implying that the deep sparse feature extraction ability widely exists in the deep learning architectures.*

4 Experiments

In the previous section, we present various findings demonstrating that CNNs can effectively function as deep sparse coding solvers, efficiently approximating sparse features. Naturally, this begs the question: Could enforcing sparsity in neural networks further enhance their performance? To evaluate the influence of sparsity on the performance of neural networks, we conduct a series of experiments on image classification and image segmentation tasks.

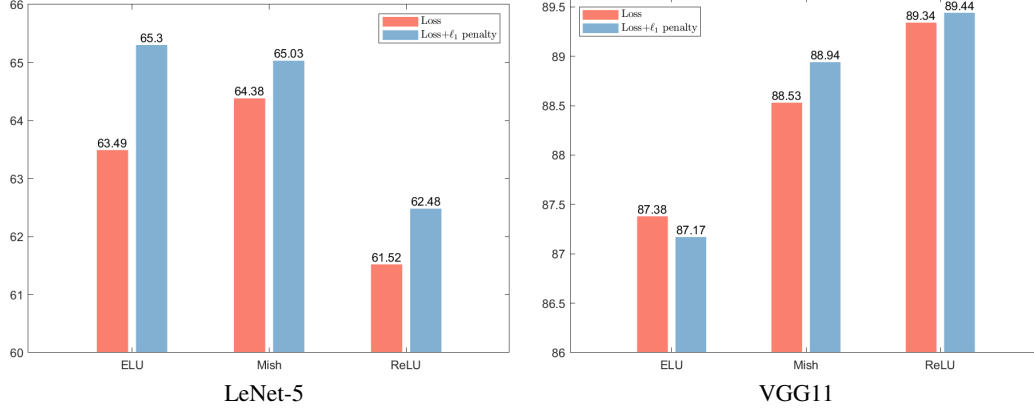


Figure 1: Test accuracy over CIFAR10.

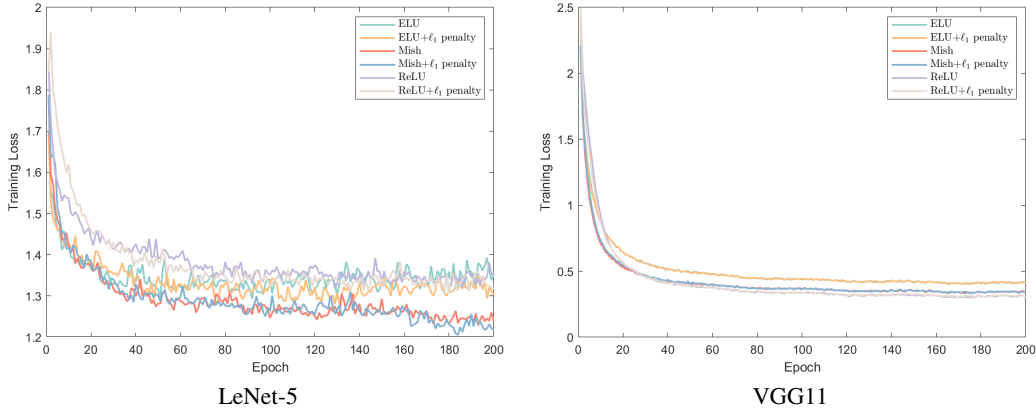


Figure 2: Training loss over CIFAR10.

Training strategy. To obtain sparser features, we introduce an ℓ_1 penalty term into the loss function. This penalty term acts as a regularization term, encouraging the network to learn sparse representations. Specifically, we modify the original loss function L as follows:

$$L_{\text{sparse}} := L + \gamma \sum_j \omega_j \|\mathbf{x}_j\|_1,$$

where \mathbf{x}_j are features of outputs of some intermediate layers, γ is the trade-off hyper-parameter, and ω_j is used to balance the sparsity of features from different layers.

In our experiments, we fix all hyper-parameters except for γ , including but not limited to network architectures, learning rates, batch size, to ensure a fair comparison. We compare the performance of the network with and without the ℓ_1 penalty term, under various evaluation metrics.

4.1 Image classification

Image classification tasks aim to classify a given image according to a predefined set of labels. In this study, we evaluate the performance of deep learning models on the CIFAR-10 dataset, a widely used benchmark for image classification. The CIFAR-10 dataset comprises 50,000 training images and 10,000 test images, spanning 10 distinct classes.

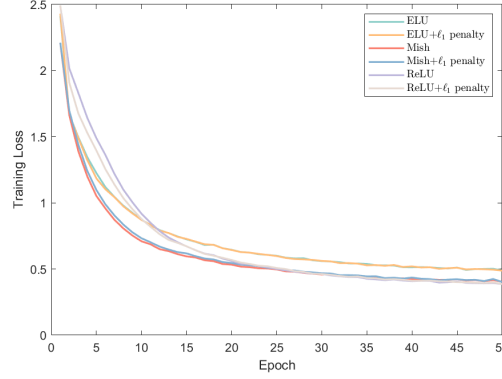


Figure 3: Training loss of VGG11 over first 50 epoch.

For the neural network architectures, we select two well-known image classification networks: LeNet-5 [6] and VGG11 [15]. LeNet-5, a pioneering convolutional neural network, contains approximately 60,000 trainable parameters, while VGG11, a deeper and more complex model, boasts over 9 million trainable parameters. These networks typically employ convolutional layers to extract discriminative features from images, followed by fully connected layers for classification. Details of structures can be found in Table 1. In their structures, we only consider to add ℓ_1 penalty of features far away from the classifiers to avoid to much impact on the prediction part.

To encourage sparsity in the extracted features, we impose an ℓ_1 penalty on the outputs of the initial convolutional layers. As demonstrated in the previous section, several activation functions, including ReLU-type functions and others, possess the ability to learn sparse feature representations in neural networks. Therefore, we investigate the performance of three distinct activation functions: ELU [3], Mish [9], and ReLU.

LeNet-5	conv5-6 + maxpool + conv5-16 + maxpool + FC120 + FC84 + FC10
VGG11	conv3-64 + maxpool + conv3-128 + maxpool + conv3-256 \times 2 + maxpool + conv3-512 \times 2 + maxpool + conv3-512 \times 2 + maxpool + avgpool + FC10

Table 1: Architectures of LeNet-5 and VGG11. The notation ‘conv5-6’ means for this convolution we set kernel size 5 and output channel 6 and ‘FC120’ means output dimension is 120. In each convolution of VGG11, we set padding to be 1 and employ batch normalization, and for LeNet-5 we set paddings to be 0. The **red** color means the outputs of corresponding blocks are considered in the ℓ_1 penalty.

During the training, we utilize the Stochastic Gradient Descent (SGD) algorithm with a minibatch size of 128. The learning rate is set using cosine annealing schedule, starting with an initial value of 0.1. We adopt the cross-entropy loss function as the objective for optimization. The training is conducted for 200 epochs. Weight decay is set to be 5×10^{-4} . We set $\omega_j := 1/\dim(\mathbf{x}_j)$ and collect the choice of γ in Table 2.

γ	ReLU	ELU	Mish
LeNet-5	10^{-3}	10^{-2}	10^{-4}
VGG11	10^{-3}	10^{-5}	10^{-3}

Table 2: The choice of γ .

The test accuracy of each model is collected in Figure 1. We can see in the most cases, ℓ_1 penalty do help improve the classification accuracy. Besides, the performance of these activation functions are all within a small range, which indicates that neural networks may work as a deep sparse coding solver no matter what activation functions are used. We further collect the training loss in Figure 2, and plot first 50 training loss in Figure 3. These figures show that for the same activation function, training losses have a similar shape, which is more clear under the VGG11 architecture. In Figure 3, we can see for the same activation function, losses decay very fast to a similar value. Together with the test accuracy, increasing the sparsity could be a safe choice for improving the performance since training loss are unlikely to change a lot.

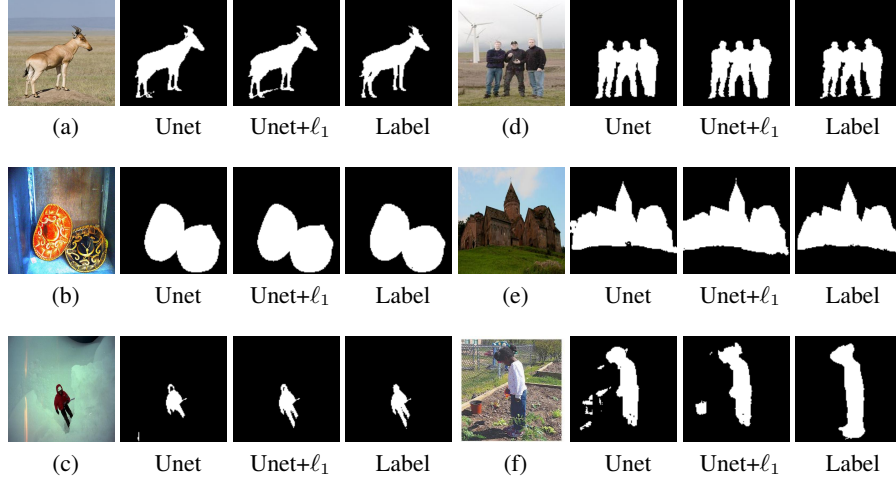


Figure 4: Segmentation results. Images (a)-(c) are from DUTS-TE and images (d)-(f) are from DUT-OMRON.

Prediction \ Label	Label	
	Positive	Negative
Positive	TP	FP
Negative	FN	TN

Table 3: Confusion Matrix.

4.2 Image segmentation

Image segmentation aims at partitioning pixels of a digital image into multiple segments. Unet [13] is one of the most well known deep network architecture to predict pixel-wise labels for image segmentation. The proposed encoding and decoding approach are frequently referred to as the U structure. Specifically, there are five encoding blocks and four decoding blocks in Unet. After it was noticed by researchers in this field, a lot of work are proposed, designing similar U structures and make neural networks great success in various fields, including computer sciences, medical imaging and many others.

In this part, we consider 2 benchmark datasets for pixel-wise binary classification: DUTS [19], DUT-OMRON [20]. DUTS has DUTS-TR for training and DUTS-TE for testing, containing 10553 and 5019 images, respectively. DUT-OMRON comprises of 5168 images for salient objective detection task. Our experiment utilizes DUTS-TR to train Unet and take others for evaluation.

During the training, we utilize the ADAM algorithm with a minibatch size of 4. The learning rate is set using cosine annealing schedule, starting with an initial value of 0.005. We adopt the Binary Cross Entropy⁴ (BCE) loss function as the objective for optimization. The training is conducted for 200 epochs and we set γ to be 10^{-3} . With respect to the penalty term in L_{sparse} , we push the features from the first four encoding blocks to have smaller ℓ_1 norm with $\omega_j := 1/\dim(\mathbf{x}_j)$.

To evaluate the performance of the prediction against the ground truth, we employ the following three measurements:

$$\begin{aligned}
 \text{PA} &:= \frac{\text{TP} + \text{TN}}{\text{TP} + \text{TN} + \text{FP} + \text{FN}}, \\
 \text{mPA} &:= \frac{1}{2} \left(\frac{\text{TP}}{\text{TP} + \text{FP}} + \frac{\text{TN}}{\text{TN} + \text{FN}} \right), \\
 \text{mIoU} &:= \frac{1}{2} \left(\frac{\text{TP}}{\text{TP} + \text{FP} + \text{FN}} + \frac{\text{TN}}{\text{TN} + \text{FP} + \text{FN}} \right).
 \end{aligned}$$

which are based on the definition of the confusion matrix Table 3.

⁴<https://pytorch.org/docs/stable/generated/torch.nn.BCELoss.html>

		PA	mPA	mIoU
DUTS-TE	Unet	0.9203±0.1004	0.8423±0.1529	0.7584±0.1840
	Unet+ ℓ_1	0.9224±0.0972	0.8446±0.1494	0.7582±0.1799
DUT-OMRON	Unet	0.9166±0.1097	0.8305±0.1749	0.7503±0.2060
	Unet+ ℓ_1	0.9209±0.1021	0.8322±0.1724	0.7524±0.2011

Table 4: Average performance and standard deviation of Unet on each dataset.

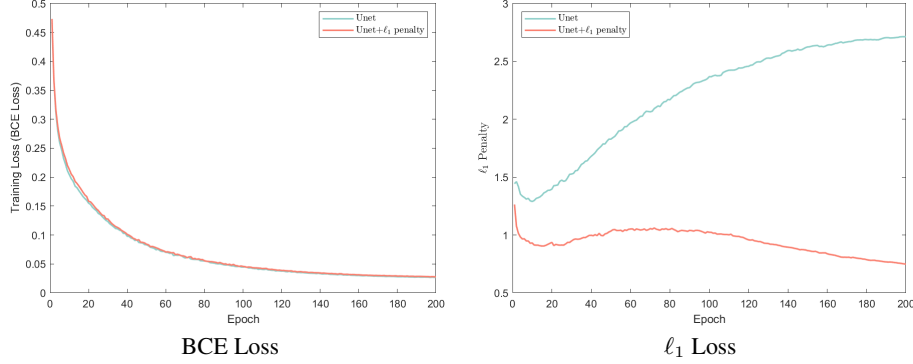
Figure 5: BCE loss and ℓ_1 penalty ($\sum_j \omega_j \|\mathbf{x}_j\|_1$) during training.

Table 4 collects the average performance of Unet on each dataset. With additional ℓ_1 penalty and keeping other hyper-parameters, the performance can be improved under the most measurements. Furthermore, the standard deviation in Table 4 unveils that improving sparsity could possibly yield a more stable model. In Figure 5, BCE loss is not greatly affected by the additional penalty term. In the meanwhile, the ℓ_1 penalty term can effectively control the ℓ_1 norm of learned features. Regarding a feature \mathbf{x}_j , we take the measurement $\|\mathcal{H}_\alpha(\mathbf{x}_j)\|_0/\dim(\mathbf{x}_j)$ to quantify the sparsity, where hard threshold \mathcal{H}_α is defined as $\mathcal{H}_\alpha(\mathbf{x}_j)_i := (\mathbf{x}_j)_i$ if $|(\mathbf{x}_j)_i| > \alpha$ and zero otherwise. We set $\alpha = 10^{-6}$ and collect sparsity results in Figure 6. As the neural network goes deeper, features become sparser. Even in Unet, features of deeper encoders have good sparsity. These results indicate that neural networks could be benefit from sparsity. We also show three segmentation results from each dataset in Figure 4.

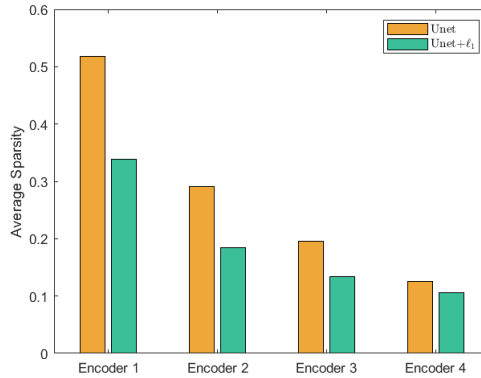


Figure 6: Average sparsity of features produced by Unet over DUT-OMRON.

5 Conclusion and future work

In this work, we have studied the ability of convolutional neural networks to learn deep sparse features. We first discussed the uniqueness and stability of deep sparse coding models under a general setting, and explored different ways to relax the required conditions. We then provided convergence analysis for approximating deep sparse features, which offers a theoretical support for the observed sparsity in the internal representations of CNNs. Additionally, we generalized our results to neural networks with various activation functions and structures, which suggests that

deep sparse feature extraction may be a widely occurring phenomenon in many popular neural network architectures. Motivated by these insights into the sparsity of CNN features, we introduced an ℓ_1 regularization strategy for training such models. Numerical experiments are conducted indicating that the ℓ_1 penalty can potentially push CNNs to extract sparser features, which in turn can improve the performance on downstream tasks.

Theoretically, the analysis of approximation and estimation errors in parametric models significantly depends on the dimensionality of the feature space. With sparsity, we anticipate that the error rate will be significantly reduced, which can be rigorously proven and will help explain the success of deep neural networks. This will be the focus of our future work.

Acknowledgments

The research and the work described in this paper was partially supported by grants from the Research Grants Council of the Hong Kong Special Administrative Region, China [Projects Nos. CityU 11303821, CityU 11315522, CityU 11308020]. The work of D. X. Zhou was partially supported by Discovery Project (DP240101919) of the Australian Research Council.

Appendix A

In the following, we first introduce results of sparse signals of linear inverse problem $\mathbf{y} = \mathbf{D}\mathbf{x}^* + \varepsilon$.

A LISTA-CP sequence $\{\mathbf{x}^{(k)}\}_{k=0}^{\infty}$ for linear inverse problem $\mathbf{y} = \mathbf{D}\mathbf{x}^* + \varepsilon$ is defined as

$$\begin{aligned}\mathbf{x}^{(0)} &:= 0, \\ \mathbf{x}^{(k+1)} &:= \mathcal{T}_{\theta^{(k)}}(\mathbf{x}^{(k)} + (\mathbf{W}^{(k)})^\top (\mathbf{y} - \mathbf{D}\mathbf{x}^{(k)})), k = 1, 2, 3, \dots,\end{aligned}\tag{6}$$

where \mathcal{T}_α is the soft thresholding function.

Given any $(\mathbf{x}^*, \varepsilon)$, the LISTA sequence $\{\mathbf{x}^{(k)}\}_{k=0}^{\infty}$ is determined. Hence we may also write $\mathbf{x}^{(k)}$ as $\mathbf{x}^{(k)}(\mathbf{x}^*, \varepsilon)$ when we emphasize the dependence. To characterize $\{(\mathbf{W}^{(k)}, \theta^{(k)})\}_{k=0}^{\infty}$, we need to utilize the concept of generalized mutual coherence.

Definition 5.1. *The generalized mutual coherence of \mathbf{A} , with each column being normalized, is given by*

$$\tilde{\mu}(\mathbf{A}) = \inf_{\mathbf{W} \in \mathbb{R}^{m \times d}, \mathbf{w}_i^\top \mathbf{a}_i = 1, i \in [d]} \left\{ \max_{i \neq j, i, j \in [d]} |\mathbf{w}_i^\top \mathbf{a}_j| \right\}.$$

The existence of \mathbf{W} that achieves the value $\tilde{\mu}(\mathbf{A})$ is guaranteed by \mathbf{A} belongs to the feasible set and the definition of $\tilde{\mu}(\mathbf{A})$ can be seen as a linear programming problem [2].

Definition 5.2. *Given \mathbf{A} , define the following set*

$$\mathcal{X}(\mathbf{A}) = \operatorname{argmin}_{\mathbf{W} \in \mathbb{R}^{m \times d}} \left\{ \max_{ij} |W_{ij}| : \mathbf{w}_i^\top \mathbf{a}_i = 1, i \in [d], \max_{i \neq j} |\mathbf{w}_i^\top \mathbf{a}_j| = \tilde{\mu}(\mathbf{A}) \right\}.$$

Theorem 5.1 (Theorem 2 [2]). *Consider a linear inverse problem $\mathbf{y} = \mathbf{D}\mathbf{x}^* + \varepsilon$ where columns of \mathbf{D} are normalized and $(\mathbf{x}^*, \varepsilon)$ satisfies Assumption 2 with $\|\mathbf{x}^*\|_0 < (1 + 1/\tilde{\mu}(\mathbf{D}))/2$. If each $(\mathbf{W}^{(k)}, \theta^{(k)})$ in $\{(\mathbf{W}^{(k)}, \theta^{(k)})\}_{k=0}^{\infty}$ satisfies*

$$\mathbf{W}^{(k)} \in \mathcal{X}(\mathbf{D}), \quad \theta^{(k)} = \sup_{(\mathbf{x}^*, \varepsilon) \in \mathbb{X}(B, \varepsilon)} \left\{ \tilde{\mu}(\mathbf{D}) \|\mathbf{x}^{(k)}(\mathbf{x}^*, \varepsilon) - \mathbf{x}^*\|_1 \right\} + C_{\mathbf{W}^{(k)}} \delta, \tag{7}$$

where $C_{\mathbf{W}^{(k)}} = \max_{i \in [m], j \in [d]} |W_{ij}^{(k)}|$, then the LISTA-CP sequence $\{\mathbf{x}^{(k)}\}_{k=0}^{\infty}$ generated by (6) for all $(\mathbf{x}^*, \varepsilon) \in \mathbb{X}(B, s, \delta)$ has the same support as \mathbf{x}^* , i.e. $\operatorname{supp} \mathbf{x}^{(k)} = \operatorname{supp} \mathbf{x}^*$ and satisfies

$$\|\mathbf{x}^{(k)}(\mathbf{x}^*, \varepsilon) - \mathbf{x}^*\|_2 \leq sBe^{-ck} + C\delta, \quad k = 1, 2, \dots$$

where $c > 0$, $C > 0$ are some constants that depend only on \mathbf{D} and $\|\mathbf{x}^*\|_0$.

Lemma 5.2 (Stability of LISTA-CP sequence). *Given \mathbf{y} , $\tilde{\mathbf{y}}$, \mathbf{D} , and $\{(\mathbf{W}^{(k)}, \theta^{(k)}) \in \mathcal{X}(\mathbf{D}) \times \mathbb{R}\}_{k=0}^{\infty}$, if the sequence $\{\mathbf{x}^{(k)}\}_{k=0}^{\infty}$ is generated by*

$$\begin{aligned}\mathbf{x}^{(0)} &:= 0, \\ \mathbf{x}^{(k+1)} &:= \mathcal{T}_{\theta^{(k)}}(\mathbf{x}^{(k)} + (\mathbf{W}^{(k)})^\top (\mathbf{y} - \mathbf{D}\mathbf{x}^{(k)})), k = 1, 2, 3, \dots,\end{aligned}$$

and the sequence $\{\tilde{\mathbf{x}}^k\}_{k=0}^\infty$ is generated by

$$\begin{aligned}\tilde{\mathbf{x}}^{(0)} &:= 0, \\ \tilde{\mathbf{x}}^{(k+1)} &:= \mathcal{T}_{\theta^{(k)}}(\tilde{\mathbf{x}}^{(k)} + (\mathbf{W}^{(k)})^\top (\tilde{\mathbf{y}} - \mathbf{D}\tilde{\mathbf{x}}^{(k)})), k = 1, 2, 3, \dots,\end{aligned}$$

then

$$\|\mathbf{x}^{(k)} - \tilde{\mathbf{x}}^{(k)}\|_2 \leq C_{\mathbf{D}} \|\mathbf{y} - \tilde{\mathbf{y}}\|_2,$$

where $C_{\mathbf{D}} > 0$ is a constant only depends on D .

Proof. Since $\|\mathcal{T}_\alpha(\mathbf{x}) - \mathcal{T}_\alpha(\tilde{\mathbf{x}})\|_2 \leq \|\mathbf{x} - \tilde{\mathbf{x}}\|_2$ for any $\mathbf{x}, \tilde{\mathbf{x}} \in \mathbb{R}^d$, we have

$$\begin{aligned}\|\mathbf{x}^{(k+1)} - \tilde{\mathbf{x}}^{(k+1)}\|_2 &\leq \left\| \left(\mathbf{I} - (\mathbf{W}^{(k)})^\top \mathbf{D} \right) (\mathbf{x}^{(k)} - \tilde{\mathbf{x}}^{(k)}) \right\|_2 + \left\| \left(\mathbf{W}^{(k)} \right)^\top (\mathbf{y} - \tilde{\mathbf{y}}) \right\|_2 \\ &\leq \left\| \mathbf{I} - (\mathbf{W}^{(k)})^\top \mathbf{D} \right\|_F \|\mathbf{x}^{(k)} - \tilde{\mathbf{x}}^{(k)}\|_2 + \|\mathbf{W}^{(k)}\|_F \|\mathbf{y} - \tilde{\mathbf{y}}\|_2 \\ &\leq d\tilde{\mu}(\mathbf{D}) \|\mathbf{x}^{(k)} - \tilde{\mathbf{x}}^{(k)}\|_2 + \sqrt{md}C_{\mathbf{W}} \|\mathbf{y} - \tilde{\mathbf{y}}\|_2 \\ &\leq (d\tilde{\mu}(\mathbf{D}))^{k+1} \|\mathbf{x}^{(0)} - \tilde{\mathbf{x}}^{(0)}\|_2 + \left(\sum_{i=0}^k d^i \tilde{\mu}(\mathbf{D})^i \right) \sqrt{md}C_{\mathbf{W}} \|\mathbf{y} - \tilde{\mathbf{y}}\|_2 \\ &\leq \frac{\sqrt{md}C_{\mathbf{W}} (d^{k+1} \tilde{\mu}(\mathbf{D})^{k+1} - 1)}{d\tilde{\mu}(\mathbf{D}) - 1} \|\mathbf{y} - \tilde{\mathbf{y}}\|_2\end{aligned}$$

where the second inequality follows from $\|\mathbf{A}\mathbf{x}\|_2 \leq \|\mathbf{A}\|_2 \|\mathbf{x}\|_2$ and $\|\mathbf{A}\|_2 \leq \|\mathbf{A}\|_F$ for any matrix $\mathbf{A} \in \mathbb{R}^{m \times d}$ and $\mathbf{x} \in \mathbb{R}^d$ and in the last inequality we use $\mathbf{x}^{(0)} = \tilde{\mathbf{x}}^{(0)}$. \square

Lemma 5.3 (CNNs realize LISTA-CP sequences). *Given $K \in \mathbb{N}$, there exists a CNN Φ with kernel size s , depth $O(K \log_s(d + m))$ and number of weights $O(K(m + d)^2)$ such that for any given LISTA-CP sequence $\{\mathbf{x}^{(k)}\}_{k=0}^K$ which is determined by $\{(\mathbf{W}^{(k)}, \theta^{(k)})\}_{k=0}^{(K)}$ and \mathbf{y} , we have $\Phi(\mathbf{y}) = \mathbf{x}^{(K)}$.*

Proof. Denote $\mathbf{I}_d \in \mathbb{R}^{d \times d}$, $\mathbf{O}_{m \times d} \in \mathbb{R}^{m \times d}$ the identity matrix and zero matrix respectively. We briefly denote $\mathbf{O}_d := \mathbf{O}_{d \times d}$ when $m = d$ and $\mathbf{0}_d := \mathbf{O}_{d \times 1}$ for simplicity. We shall use $\mathbf{1}_d := (1)_{i \in [d]}$ to represent constant 1 vectors.

First of all, the shrinkage operator \mathcal{T}_α can be expressed by ReLU $\delta(x) = \max\{x, 0\}$ as

$$\begin{aligned}\mathcal{T}_\alpha(\mathbf{x}) &= \delta(\mathbf{x} - \alpha \mathbf{1}_d) - \delta(-\mathbf{x} - \alpha \mathbf{1}_d) \\ &= (\mathbf{I}_d, -\mathbf{I}_d) \delta \left(\begin{pmatrix} \mathbf{I}_d \\ -\mathbf{I}_d \end{pmatrix} \mathbf{x} - \alpha \begin{pmatrix} \mathbf{1}_d \\ \mathbf{1}_d \end{pmatrix} \right), \quad \forall \mathbf{x} \in \mathbb{R}^d.\end{aligned}$$

Then the definition (6) of $\mathbf{x}^{(k+1)}$ implies

$$\begin{aligned}\mathbf{x}^{(k+1)} &= \mathcal{T}_{\theta^{(k)}} \left(\begin{pmatrix} \mathbf{I}_d - (\mathbf{W}^{(k)})^\top \mathbf{D} & (\mathbf{W}^{(k)})^\top \end{pmatrix} \begin{pmatrix} \mathbf{x}^{(k)} \\ \mathbf{y} \end{pmatrix} \right) \\ &= (\mathbf{I}_d, -\mathbf{I}_d) \delta \left(\begin{pmatrix} \mathbf{I}_d \\ -\mathbf{I}_d \end{pmatrix} \begin{pmatrix} \mathbf{I}_d - (\mathbf{W}^{(k)})^\top \mathbf{D} & (\mathbf{W}^{(k)})^\top \end{pmatrix} \begin{pmatrix} \mathbf{x}^{(k)} \\ \mathbf{y} \end{pmatrix} - \theta^{(k)} \begin{pmatrix} \mathbf{1}_d \\ \mathbf{1}_d \end{pmatrix} \right) \\ &= (\mathbf{I}_d, -\mathbf{I}_d) \delta \left(\begin{pmatrix} \mathbf{I}_d - (\mathbf{W}^{(k)})^\top \mathbf{D} & (\mathbf{W}^{(k)})^\top \\ -\mathbf{I}_d + (\mathbf{W}^{(k)})^\top \mathbf{D} & -(\mathbf{W}^{(k)})^\top \end{pmatrix} \begin{pmatrix} \mathbf{x}^{(k)} \\ \mathbf{y} \end{pmatrix} - \theta^{(k)} \begin{pmatrix} \mathbf{1}_d \\ \mathbf{1}_d \end{pmatrix} \right).\end{aligned}$$

Thus we have for $k > 1$,

$$\begin{aligned}\begin{pmatrix} \mathbf{x}^{(k+1)} \\ \mathbf{y} \end{pmatrix} &= \begin{pmatrix} \mathbf{I}_d & -\mathbf{I}_d & \mathbf{O}_m \\ \mathbf{O}_d & \mathbf{O}_d & \mathbf{I}_m \end{pmatrix} \delta \left(\begin{pmatrix} \mathbf{I}_d - (\mathbf{W}^{(k)})^\top \mathbf{D} & (\mathbf{W}^{(k)})^\top \\ -\mathbf{I}_d + (\mathbf{W}^{(k)})^\top \mathbf{D} & -(\mathbf{W}^{(k)})^\top \end{pmatrix} \begin{pmatrix} \mathbf{x}^{(k)} \\ \mathbf{y} \end{pmatrix} - \begin{pmatrix} \theta^{(k)} \mathbf{1}_d \\ \theta^{(k)} \mathbf{1}_d \end{pmatrix} \right) + \begin{pmatrix} \mathbf{0}_d \\ \mathbf{0}_d \\ -M \mathbf{1}_m \end{pmatrix} \\ &:= \mathbf{A}_k \delta \left(\mathbf{B}_k \begin{pmatrix} \mathbf{x}^{(k)} \\ \mathbf{y} \end{pmatrix} - \mathbf{c}_k \right) + \mathbf{e}_k,\end{aligned}$$

where $\mathbf{A}_k \in \mathbb{R}^{2d \times (2d+m)}$, $\mathbf{B}_k \in \mathbb{R}^{(2d+m) \times (d+m)}$, $\mathbf{c}_k, \mathbf{e}^{(k)} \in \mathbb{R}^{2d+m}$, and $M := \max\{|y_i| : \mathbf{y} = \mathbf{D}\mathbf{x}^* + \boldsymbol{\varepsilon}, (\mathbf{x}^*, \boldsymbol{\varepsilon}) \in \mathbb{X}(B, s, \delta)\}$.

For $k = 1$, we have $\mathbf{x}^{(1)} = \mathcal{T}_{\theta^{(0)}}((\mathbf{W}^{(0)})^\top \mathbf{y})$ and hence

$$\begin{aligned} \begin{pmatrix} \mathbf{x}^{(1)} \\ \mathbf{y} \end{pmatrix} &= \begin{pmatrix} \mathbf{I}_d & -\mathbf{I}_d & \mathbf{O}_m \\ \mathbf{O}_d & \mathbf{O}_d & \mathbf{I}_m \end{pmatrix} \delta \left(\begin{pmatrix} (\mathbf{W}^{(0)})^\top \\ -(\mathbf{W}^{(0)})^\top \\ \mathbf{I}_m \end{pmatrix} \mathbf{y} - \begin{pmatrix} \theta^{(0)} \mathbf{1}_d \\ \theta^{(0)} \mathbf{1}_d \\ -M \mathbf{1}_m \end{pmatrix} \right) + \begin{pmatrix} \mathbf{0}_d \\ \mathbf{0}_d \\ -M \mathbf{1}_m \end{pmatrix} \\ &:= \mathbf{A}_1 \delta(\mathbf{B}_1 \mathbf{y} - \mathbf{c}_1) + \mathbf{e}_k, \end{aligned}$$

where $\mathbf{A}_1 \in \mathbb{R}^{2d \times (2d+m)}$, $\mathbf{B}_1 \in \mathbb{R}^{(2d+m) \times m}$, $\mathbf{c}_k, \mathbf{e}^{(k)} \in \mathbb{R}^{2d+m}$.

By [7], it is easy to see that each \mathbf{A}_k can be realized by a CNN with depth $O(\log_2(d+m))$ and number of weights $O(d^2 + dm)$ and each \mathbf{B}_k can be realized by a CNN with depth $O(\log_2 m)$ and number of weights $O(m^2 + dm)$. Concatenating these CNNs together, we obtain a CNN Φ with depth $O(K \log_2(d+m))$ and number of weights $O(K(m+d)^2)$ such that $\Phi(\mathbf{y}) = \mathbf{x}^{(K)}$. \square

Proof of Theorem 3.1. Since $(\mathbf{x}_1, \boldsymbol{\varepsilon}_1) \in \mathbb{X}(B_1, \delta_1)$ and Assumption 1 is satisfied, Theorem 5.1 and Lemma 5.3 imply that there exists a CNN Φ_1 with depth $O(K \lceil \log d_1 \rceil)$ such that $\|\Phi_1(\mathbf{y}) - \mathbf{x}_1\|_2 \leq \lambda_1 B e^{-cK} + C_1 \delta_1$ for some constants $c, C > 0$. We denote $\tilde{\mathbf{x}}_1^{(K)} = \Phi_1(\mathbf{y})$. For the linear inverse problem $\mathbf{x}_1 = \mathbf{D}_2 \mathbf{x}_2 + \boldsymbol{\varepsilon}_2$, since $(\mathbf{x}_2, \boldsymbol{\varepsilon}_2) \in \mathbb{X}(B_2, \delta_2)$ and $\|\mathbf{x}_2\|_0 \leq \lambda_2$, using Theorem 5.1, there exists a LISTA-CP sequence $\{\mathbf{x}_2^{(k)}\}_{k=0}^{(K)}$ such that $\|\mathbf{x}_2^{(K)} - \mathbf{x}_2\|_2 \leq \lambda_2 B_2 e^{-cK} + C_2 \delta_2$. By Lemma 5.2, there exists Φ_2 such that $\Phi_2(\mathbf{x}_1) = \mathbf{x}_2^{(K)}$ and

$$\begin{aligned} \|\Phi_2 \circ \Phi_1(\mathbf{y}) - \mathbf{x}_2\|_2 &\leq \|\Phi_2(\tilde{\mathbf{x}}_1^{(K)}) - \Phi_2(\mathbf{x}_1)\|_2 + \|\Phi_2(\mathbf{x}_1) - \mathbf{x}_2\|_2 \\ &\leq C_{\mathbf{D}_2} \lambda_1 B_1 e^{-cK} + C_{\mathbf{D}_2} C_1 \delta_1 + \lambda_2 B_2 e^{-cK} + C_2 \delta_2. \end{aligned}$$

Iteratively, we are able to show the claim. \square

Appendix B

In the following, we generalize Theorem 5.1 to general activation functions. The main idea of the proof is inspired by Theorem 2 [2].

Theorem 5.4. Consider the sparse coding problem $\mathbf{y} = \mathbf{D}\mathbf{x}^* + \boldsymbol{\varepsilon}$ and assume that $\|\mathbf{x}^*\|_0 = |\mathcal{S}| < \frac{1}{2-2L} \left(\frac{1}{\mu} - 2Ld \right)$. Let the sequence $\{\mathbf{x}^{(k)}\}_{k=0}^\infty$ be generated from the following iteration

$$\mathbf{x}^{(k+1)} = \rho \left(\mathbf{x}^{(k)} + (\mathbf{W}^{(k)})^T (\mathbf{y} - \mathbf{D}\mathbf{x}^{(k)}) - \theta_k \mathbf{1} \right) - \rho \left(-\mathbf{x}^{(k)} - (\mathbf{W}^{(k)})^T (\mathbf{y} - \mathbf{D}\mathbf{x}^{(k)}) - \theta_k \mathbf{1} \right),$$

for $\mathbf{x}^{(0)} = \mathbf{0}$, where $\mathbf{W}^{(k)}$ and $\theta^{(k)}$ are defined in (7). Then, for any given $(\mathbf{x}^*, \boldsymbol{\varepsilon}) \in \mathcal{X}(B, \sigma)$, we have

$$\sup_{(\mathbf{x}^*, \boldsymbol{\varepsilon}) \in \mathcal{X}(B, \sigma)} \|\mathbf{x}^{(k+1)} - \mathbf{x}^*\|_1 \leq s B e^{-c(k+1)} + C \delta,$$

for some positive constants c, C .

Proof. Denote $\rho(x) = \sigma(x) + h(x)$, where $\sigma(x)$ is ReLU and $h(x) = 0$ if $x \geq 0$ and $|h(x)| \leq \beta$ if $x < 0$ with some $\beta > 0$.

Observing that

$$\begin{aligned} x_i^{(k)} + (\mathbf{w}_i^{(k)})^T (\mathbf{y} - \mathbf{D}\mathbf{x}^{(k)}) &= x_i^{(k)} - (\mathbf{w}_i^{(k)})^T \mathbf{D}(\mathbf{x}^{(k)} - \mathbf{x}^*) + (\mathbf{w}_i^{(k)})^T \boldsymbol{\varepsilon} \\ &= x_i^{(k)} - \sum_{j=1}^d (\mathbf{w}_i^{(k)})^T \mathbf{d}_j (x_j^{(k)} - x_j^*) + (\mathbf{w}_i^{(k)})^T \boldsymbol{\varepsilon} \\ &= x_i^{(k)} - \sum_{j \neq i} (\mathbf{w}_i^{(k)})^T \mathbf{d}_j (x_j^{(k)} - x_j^*) - (x_i^{(k)} - x_i^*) + (\mathbf{w}_i^{(k)})^T \boldsymbol{\varepsilon} \\ &= x_i^* - \sum_{j \neq i} (\mathbf{w}_i^{(k)})^T \mathbf{d}_j (x_j^{(k)} - x_j^*) + (\mathbf{w}_i^{(k)})^T \boldsymbol{\varepsilon}, \end{aligned} \tag{8}$$

and fixing an $i \notin \sigma$, i.e. $x_i^* = 0$, we have the following inequalities hold

$$\begin{aligned}
& \left| x_i^{(k)} + (\mathbf{w}_i^{(k)})^T (\mathbf{y} - \mathbf{D}\mathbf{x}^{(k)}) \right| \\
&= \left| - \sum_{j \neq i} (\mathbf{w}_i^{(k)})^T \mathbf{d}_j (x_j^{(k)} - x_j^*) + (\mathbf{w}_i^{(k)})^T \varepsilon \right| \\
&\leq \tilde{\mu} \|\mathbf{x}^{(k)} - \mathbf{x}^*\|_1 + C_{\mathbf{W}} \delta \\
&\leq \theta^{(k)}.
\end{aligned} \tag{9}$$

For simplicity, let us denote

$$H(\mathbf{x}^{(k)}; \mathbf{W}^{(k)}, \theta^{(k)})_i = h(\mathbf{x}_i^{(k)} + (\mathbf{w}_i^{(k)})^T (\mathbf{y} - \mathbf{D}\mathbf{x}^{(k)}) - \theta^{(k)}) - h(-\mathbf{x}_i^{(k)} - (\mathbf{w}_i^{(k)})^T (\mathbf{y} - \mathbf{D}\mathbf{x}^{(k)}) - \theta^{(k)}).$$

Then, using (9), for any fixed $i \notin \sigma$, we have

$$\begin{aligned}
|x_i^{(k+1)} - x_i^*| &= \left| \sigma \left(x_i^{(k)} + (\mathbf{w}_i^{(k)})^T (\mathbf{y} - \mathbf{D}\mathbf{x}^{(k)}) - \theta^{(k)} \right) - \sigma \left(-x_i^{(k)} - (\mathbf{w}_i^{(k)})^T (\mathbf{y} - \mathbf{D}\mathbf{x}^{(k)}) - \theta^{(k)} \right) \right| \\
&\quad + \left| H(\mathbf{x}^{(k)}; \mathbf{W}^{(k)}, \theta^{(k)})_i \right| \\
&\leq \left| \mathcal{T}_{\theta^{(k)}} \left(x_i^{(k)} + (\mathbf{w}_i^{(k)})^T (\mathbf{y} - \mathbf{D}\mathbf{x}^{(k)}) \right) \right| + 2L\theta^{(k)} \\
&= 2L\theta^{(k)}.
\end{aligned} \tag{10}$$

Accoding to (8), we are able to represent $\mathbf{x}^{(k+1)}$ as

$$x_i^{(k+1)} = \mathcal{T}_{\theta^{(k)}} \left(x_i^* - \sum_{j \neq i} (\mathbf{w}_i^{(k)})^T \mathbf{d}_j (x_j^{(k)} - x_j^*) + (\mathbf{w}_i^{(k)})^T \varepsilon \right) + H(\mathbf{x}_i^{(k)}; \mathbf{W}^{(k)}, \theta^{(k)})_i$$

Define the sub-gradient $\partial \ell_1(x)$ by

$$\partial \ell_1(x) = \begin{cases} \text{sign}(x), & x \neq 0, \\ [-1, 1], & x = 0. \end{cases}$$

Then by (8), we have for any i ,

$$\begin{aligned}
x_i^{(k+1)} &\in x_i^* - \sum_{j \neq i} (\mathbf{w}_i^{(k)})^T \mathbf{d}_j (x_j^{(k)} - x_j^*) + (\mathbf{w}_i^{(k)})^T \varepsilon \\
&\quad + \theta^{(k)} \partial \ell_1 \left(x_i^{(k+1)} - H(\mathbf{x}^{(k)}; \mathbf{W}^{(k)}, \theta^{(k)})_i \right) + H(\mathbf{x}^{(k)}; \mathbf{W}^{(k)}, \theta^{(k)})_i,
\end{aligned}$$

or equivalently,

$$\begin{aligned}
x_i^{(k+1)} - x_i^* &\in - \sum_{j \neq i} (\mathbf{w}_i^{(k)})^T \mathbf{d}_j (x_j^{(k)} - x_j^*) + (\mathbf{w}_i^{(k)})^T \varepsilon \\
&\quad + \theta^{(k)} \partial \ell_1 \left(x_i^{(k+1)} - H(\mathbf{x}^{(k)}; \mathbf{W}^{(k)}, \theta^{(k)})_i \right) + H(\mathbf{x}^{(k)}; \mathbf{W}^{(k)}, \theta^{(k)})_i.
\end{aligned} \tag{11}$$

which implies

$$\left| x_i^{(k+1)} - x_i^* \right| \leq \left| \sum_{j \neq i} (\mathbf{w}_i^{(k)})^T \mathbf{d}_j (x_j^{(k)} - x_j^*) \right| + C_{\mathbf{W}} \delta + \theta^{(k)} + 2\beta.$$

Hence, applying (11) for $i \in \mathcal{S}$ and (10) $i \notin \mathcal{S}$, we obtain

$$\begin{aligned}
\|\mathbf{x}^{(k+1)} - \mathbf{x}^*\|_1 &= \sum_{i \in \sigma} |x_i^{(k+1)} - x_i^*| + \sum_{i \notin \sigma} |x_i^{(k+1)}| \\
&\leq \tilde{\mu} \sum_{i \in \sigma} \sum_{j \neq i} |x_j^{(k)} - x_j^*| + 2L(d - |\mathcal{S}|)\theta^{(k)} + |\sigma|C_{\mathbf{W}}\delta + |\sigma|\theta^{(k)} + 2|\mathcal{S}|\beta \\
&\leq \tilde{\mu}|\mathcal{S}| \|\mathbf{x}^{(k)} - \mathbf{x}^*\|_1 + (2Ld + (1 - 2L)|\mathcal{S}|)\theta^{(k)} + |\sigma|C_{\mathbf{W}}\delta + 2|\mathcal{S}|\beta.
\end{aligned}$$

Replacing the definition (7) of $\theta^{(k)}$ in the above inequalities, we immediately derive

$$\begin{aligned} \sup_{(\mathbf{x}^*, \epsilon) \in \mathbb{X}(B, \epsilon)} \|\mathbf{x}^{(k+1)} - \mathbf{x}^*\|_1 &\leq \tilde{\mu} (2Ld + (2 - 2L)|\sigma|) \sup_{(\mathbf{x}^*, \epsilon) \in \mathbb{X}(B, \epsilon)} \|\mathbf{x}^{(k)} - \mathbf{x}^*\|_1 \\ &\quad + (2Ld + (2 - 2L)|\sigma|) C_{\mathbf{W}} \delta + 2|\mathcal{S}| \beta. \end{aligned} \quad (12)$$

Denote $\alpha := \tilde{\mu} (2Ld + (2 - 2L)|\sigma|)$. By induction for (12), we obtain

$$\sup_{(\mathbf{x}^*, \epsilon) \in \mathbb{X}(B, \epsilon)} \|\mathbf{x}^{(k+1)} - \mathbf{x}^*\|_1 \leq \alpha^{k+1} \sup_{(\mathbf{x}^*, \epsilon) \in \mathbb{X}(B, \epsilon)} \|\mathbf{x}^{(0)} - \mathbf{x}^*\|_1 + (\alpha C_{\mathbf{W}} \delta + 2|\mathcal{S}| \beta) \sum_{i=0}^k \alpha^i.$$

Hence, when $\|\mathbf{x}^*\|_0 = |\mathcal{S}| < \frac{1}{2-2L} \left(\frac{1}{\tilde{\mu}} - 2Ld \right)$, then there exists $c := -\ln \alpha > 0$ such that $\alpha^k = e^{-ck}$. \square

Proof of Theorem 3.4. We can use the similar idea in Theorem 3.1 to prove this result since except for Theorem 5.1, Theorem 3.1 is mainly established on Lemma 5.2 and Lemma 5.3. We can obtain a similar result as Lemma 5.2 by using Lipschitz condition of ρ and for Lemma 5.3, it rewrites the sequence and Theorem 1 in [7] also holds for ρ due to its positive part. Notice that for any positive integer m , the following properties hold

- (a) $|\rho^m(0)| = 0$ and $\rho^m(x) = x$ for $x \geq 0$;
- (b) $|\rho^m(x) - \rho^m(y)| \leq L^{m-1}|x - y|$;
- (c) $|\rho^m(x)| = |\rho^m(x) - \rho^m(0)| \leq L|\rho^{m-1}(x) - \rho^{m-1}(0)| \leq \dots \leq L^{m-1}|\rho(x) - \rho(0)| \leq L^{m-1}\beta$

Hence using ρ^k as the activation function in Theorem 5.4, we can get our result. \square

Proof of Theorem 3.5. Let us first prove the error between the following sequences

$$\begin{aligned} \mathbf{x}^{(k+1)} &= \sigma \left(\mathbf{A}_1^{(k)} \mathbf{x}^{(k)} + \mathbf{A}_2^{(k)} \mathbf{y} + \mathbf{b}^{(k)} \right), \\ \tilde{\mathbf{x}}^{(k+1)} &= \phi_\rho \left(\mathbf{A}_1^{(k)} \tilde{\mathbf{x}}^{(k)} + \mathbf{A}_2^{(k)} \mathbf{y} + \mathbf{b}^{(k)} \right), \end{aligned}$$

where $\tilde{\mathbf{x}}^{(0)} = \mathbf{x}^{(0)} = \mathbf{0}$. Then we have

$$\begin{aligned} \|\mathbf{x}^{(k+1)} - \tilde{\mathbf{x}}^{(k+1)}\|_\infty &\leq \left\| \sigma \left(\mathbf{A}_1^{(k)} \mathbf{x}^{(k)} + \mathbf{A}_2^{(k)} \mathbf{y} + \mathbf{b}^{(k)} \right) - \sigma \left(\mathbf{A}_1^{(k)} \tilde{\mathbf{x}}^{(k)} + \mathbf{A}_2^{(k)} \mathbf{y} + \mathbf{b}^{(k)} \right) \right\|_\infty \\ &\quad + \left\| \sigma \left(\mathbf{A}_1^{(k)} \tilde{\mathbf{x}}^{(k)} + \mathbf{A}_2^{(k)} \mathbf{y} + \mathbf{b}^{(k)} \right) - \phi_\rho \left(\mathbf{A}_1^{(k)} \tilde{\mathbf{x}}^{(k)} + \mathbf{A}_2^{(k)} \mathbf{y} + \mathbf{b}^{(k)} \right) \right\|_\infty \\ &\leq \|\mathbf{A}_1^{(k)}\|_\infty \|\mathbf{x}^{(k)} - \tilde{\mathbf{x}}^{(k)}\|_\infty + \varepsilon. \end{aligned}$$

By induction, we have

$$\begin{aligned} \|\mathbf{x}^{(k+1)} - \tilde{\mathbf{x}}^{(k+1)}\|_\infty &\leq \prod_{i=0}^k \|\mathbf{A}_1^{(i)}\|_\infty \|\mathbf{x}^{(0)} - \tilde{\mathbf{x}}^{(0)}\|_\infty + \varepsilon \sum_{i=0}^k \prod_{j=0}^i \|\mathbf{A}_1^{(k-j)}\|_\infty \\ &\leq \varepsilon \sum_{i=0}^k \prod_{j=0}^i \|\mathbf{A}_1^{(k-j)}\|_\infty. \end{aligned}$$

Let us choose $\mathbf{A}_1^{(k)} := \mathbf{I} - (\mathbf{W}^{(k)})^\top \mathbf{D}$ for some $\mathbf{D} \in \mathbb{R}^{m \times d}$. According to the definition of $\mathbf{W}^{(k)}$, one can direct get the upper bound of $\|\mathbf{A}_1^{(k)}\|_\infty \leq (d-1)\tilde{\mu}(\mathbf{D})$. Together with Theorem 3.1, we complete the proof. \square

References

- [1] Aviad Aberdam, Jeremias Sulam, and Michael Elad. Multi-layer sparse coding: The holistic way. *SIAM Journal on Mathematics of Data Science*, 1(1):46–77, 2019.
- [2] Xiaohan Chen, Jialin Liu, Zhangyang Wang, and Wotao Yin. Theoretical linear convergence of unfolded ISTA and its practical weights and thresholds. *Advances in Neural Information Processing Systems*, 31, 2018.
- [3] Djork-Arné Clevert, Thomas Unterthiner, and Sepp Hochreiter. Fast and accurate deep network learning by exponential linear units (ELUs). In *International Conference on Learning Representations (ICLR)*, pages 1–14, 2016.
- [4] Jean-Baptiste Cordonnier, Andreas Loukas, and Martin Jaggi. On the relationship between self-attention and convolutional layers. In *International Conference on Learning Representations (ICLR)*, 2020.
- [5] Michael Elad. *Sparse and redundant representations: from theory to applications in signal and image processing*. Springer Science & Business Media, 2010.
- [6] Y. Lecun, L. Bottou, Y. Bengio, and P. Haffner. Gradient-based learning applied to document recognition. *Proceedings of the IEEE*, 86(11):2278–2324, 1998.
- [7] Jianfei Li, Han Feng, and Ding-Xuan Zhou. Approximation analysis of CNNs from a feature extraction view. *Analysis and Applications*, 22(03):635–654, 2024.
- [8] Tong Mao, Zhongjie Shi, and Ding-Xuan Zhou. Approximating functions with multi-features by deep convolutional neural networks. *Analysis and Applications*, 21(01):93–125, 2023.
- [9] Diganta Misra. Mish: A self regularized non-monotonic neural activation function. *arXiv*, abs/1908.08681, 2019.
- [10] Thanh V Nguyen, Raymond KW Wong, and Chinmay Hegde. Provably accurate double-sparse coding. *Journal of Machine Learning Research*, 20(141):1–43, 2019.
- [11] Vardan Papyan, Yaniv Romano, and Michael Elad. Convolutional neural networks analyzed via convolutional sparse coding. *Journal of Machine Learning Research*, 18(1):2887–2938, 2017.
- [12] Ives Rey-Otero, Jeremias Sulam, and Michael Elad. Variations on the convolutional sparse coding model. *IEEE Transactions on Signal Processing*, 68:519–528, 2020.
- [13] Olaf Ronneberger, Philipp Fischer, and Thomas Brox. U-net: Convolutional networks for biomedical image segmentation. In *Medical image computing and computer-assisted intervention–MICCAI 2015: 18th international conference, Munich, Germany, October 5–9, 2015, proceedings, part III 18*, pages 234–241. Springer, 2015.
- [14] Ron Rubinstein, Michael Zibulevsky, and Michael Elad. Double sparsity: Learning sparse dictionaries for sparse signal approximation. *IEEE Transactions on Signal Processing*, 58(3):1553–1564, 2010.
- [15] Karen Simonyan and Andrew Zisserman. Very deep convolutional networks for large-scale image recognition. *arXiv.org*, 2015.
- [16] Jeremias Sulam, Aviad Aberdam, Amir Beck, and Michael Elad. On multi-layer basis pursuit, efficient algorithms and convolutional neural networks. *IEEE Transactions on Pattern Analysis and Machine Intelligence*, 42(8):1968–1980, 2019.
- [17] Jeremias Sulam, Vardan Papyan, Yaniv Romano, and Michael Elad. Multilayer convolutional sparse modeling: Pursuit and dictionary learning. *IEEE Transactions on Signal Processing*, 66(15):4090–4104, 2018.
- [18] Ashish Vaswani, Noam Shazeer, Niki Parmar, Jakob Uszkoreit, Llion Jones, Aidan N Gomez, Łukasz Kaiser, and Illia Polosukhin. Attention is all you need. *Advances in Neural Information Processing Systems*, 30, 2017.
- [19] Lijun Wang, Huchuan Lu, Yifan Wang, Mengyang Feng, Dong Wang, Baocai Yin, and Xiang Ruan. Learning to detect salient objects with image-level supervision. In *2017 IEEE Conference on Computer Vision and Pattern Recognition (CVPR)*, pages 3796–3805, 2017.
- [20] Chuan Yang, Lihe Zhang, Huchuan Lu, Xiang Ruan, and Ming-Hsuan Yang. Saliency detection via graph-based manifold ranking. In *2013 IEEE Conference on Computer Vision and Pattern Recognition (CVPR)*, pages 3166–3173, 2013.
- [21] Matthew D. Zeiler, Dilip Krishnan, Graham W. Taylor, and Rob Fergus. Deconvolutional networks. In *2010 IEEE Computer Society Conference on Computer Vision and Pattern Recognition*, pages 2528–2535, 2010.
- [22] Zhiyang Zhang and Shihua Zhang. Towards understanding residual and dilated dense neural networks via convolutional sparse coding. *National Science Review*, 8(3):nwaa159, 2021.
- [23] Ding-Xuan Zhou. Deep distributed convolutional neural networks: Universality. *Analysis and applications*, 16(06):895–919, 2018.
- [24] Ding-Xuan Zhou. Universality of deep convolutional neural networks. *Applied and computational harmonic analysis*, 48(2):787–794, 2020.